AIMS Mathematics, 11(11): 39355–39385.
DOI: 10.3934/math.20261515
Received: 23 September 2026
Revised: 11 November 2026
Accepted: 13 November 2026
Published: 25 November 2026

https://www.aimspress.com/journal/Math

*Research article*

# DES-NSGA-II: Dynamic environmental selection with robust adaptive pressure and hierarchical niching

**Renyun Liu[1], Siyi Gong[1,*], Du Cheng[2], Rui Bao[1], and Yifei Yao[3]**

[1] College of Mathematics, Changchun Normal University, Changchun 130032, Jilin, China

[2] College of Artificial Intelligence, Jilin University, Changchun 130012, Jilin, China

[3] College of Computer Science and Technology, Changchun Normal University, Changchun 130032, Jilin, China

* **Correspondence:** Email: 15568964560@163.com; Tel:+86-15568964560.

**Abstract:** The Nondominated Sorting Genetic Algorithm II (NSGA-II) suffers from weakened selection pressure, limited population-state awareness, and local aggregation of solutions in many-objective optimization. This paper proposes DES-NSGA-II, a dynamic environmental selection that recasts environmental selection as a population-state-driven feedback process. A robust distribution-disturbance signal $S_1$, based on the median and interquartile range of the perpendicular distances within the truncation front, and a convergence-discrepancy signal $S_2$, derived from the first and last nondominated fronts, jointly drive a selection pressure $\beta_t$, whose mapping is bounded by construction ($1 \leq \beta_t < 2$) and smoothed across generations. A two-stage hierarchical niching mechanism then exploits this pressure: the first stage builds a convergence-oriented skeleton, and the second rewards directional novelty relative to it. On the DTLZ, WFG and MaF suites ($M \in \{3, 5, 10, 15\}$, 30 independent runs), DES-NSGA-II attains the best average IGD rank over 84 instance–dimension blocks (1.929) and the best rank on each suite (1.607, 1.821 and 2.357), with the largest margins on the regular DTLZ and WFG fronts and at $M \geq 10$. On MaF, it outperforms FDV on 23 of the 28 instances, while FDV remains the stronger method on the disconnected MaF3 front. Ablation shows that the benefit of adaptive pressure and hierarchical niching is problem- and dimension-dependent, and the limitations that remain on irregular and disconnected fronts motivate further work on geometric representation.

**Keywords:** many-objective optimization; NSGA-II; dynamic environmental selection; adaptive selection pressure; hierarchical niching; population-state feedback
**Mathematics Subject Classification:** 90C29, 68T20

## Abbreviations

| | |
|---|---|
| NSGA-II | nondominated sorting genetic algorithm II |
| DES-NSGA-II | dynamic environmental selection based on NSGA-II |
| IQR | interquartile range |
| IGD | inverted generational distance |
| $IGD^+$ | inverted generational distance plus |
| DTLZ | Deb–Thiele–Laumanns–Zitzler |
| WFG | Walking Fish Group |
| MaF | many-objective functions |
| DGEA | the compared large-scale multi-objective evolutionary algorithm of He et al. [30] |

## 1. Introduction

Many-objective optimization problems (MaOPs) arise in engineering design, scheduling, resource allocation, and other complex decision-making tasks in which a relatively large number of conflicting objectives must be optimized simultaneously. As the number of objectives grows, the proportion of mutually nondominated solutions increases rapidly, which weakens the selection pressure of Pareto dominance and makes a well-converged, well-distributed approximation hard to attain [1, 2]. Conventional diversity measures such as crowding distance also lose discriminative power in high-dimensional objective spaces [1, 3]*. Environmental selection is therefore the central difficulty of many-objective evolutionary optimization: a mechanism that works for two or three objectives may fail once the population is dominated by a single nondominated front.

NSGA-II combines fast nondominated sorting with the crowding distance and balances convergence and diversity well for low- and medium-dimensional problems [4]. As the number of objectives increases, however, a large part of the population may belong to the first nondominated front: ranking then supplies little pressure, and crowding distance can no longer separate individuals in high-dimensional objective spaces [1, 2].

A major line of research introduces reference structures into environmental selection. NSGA-III embeds predefined reference points into the sorting framework of NSGA-II [5, 6], RVEA guides the search with reference vectors and an angle-based criterion [7], and MOEA/D decomposes the problem into scalar subproblems attached to weight vectors [8]; hybrid dominance-decomposition and hyperplane-assisted schemes further enrich this line [9, 10]. These methods improve distributional coverage, but their reference structures are predefined or updated by relatively fixed rules, so that on irregular, disconnected or degenerated fronts a fixed structure may allocate directions to regions containing no Pareto-optimal solution or fail to cover regions where solutions concentrate [11–14]. The reference frame is thus improved, while the intensity of environmental selection itself remains governed by a fixed dominance or scalarizing rule.

Adaptive reference-vector and reference-direction methods address the first half of this problem.

*Part of the references predate 2020 because they are the primary sources of the operators, the reference-direction families and the performance indicators compared here; recent journal treatments of the same topics are cited alongside them. Only the $IGD^+$ definition is cited from conference proceedings, since that is its sole source, and its behavior is analyzed further in the journal survey of [14].

Liu et al. let reference vectors and scalarizing functions follow irregular fronts through a growing neural gas network [11], and later work coordinated the adaptation of both components [12, 13]. Wang et al. adjusted reference directions across evolutionary stages under a modified dominance relation [15], and Xu et al. estimated front density to steer adaptive reference vectors [16]. These methods align the reference structure with the population geometry, yet the adaptation is applied to the reference structure itself: the truncation of the last front is still decided by dominance or scalarization, so the selection intensity does not respond to the instantaneous distributional state. Adapting the frame alone cannot restore pressure when the truncation front itself becomes geometrically unstable.

A parallel line separates convergence-oriented from diversity-oriented selection. Sun et al. first emphasized convergence and then promoted diversity [17], and more recent variants combined enhanced dominance relations with separate convergence and diversity controls [15, 18]. They showed that splitting the selection stage improves the balance between the two goals, but the diversity-enhancement stage usually carries a fixed weight, which is too aggressive when the population is already well-covered and too weak when the truncation front is locally aggregated.

Angle-based and niching-based mechanisms offer a complementary view. Angle niching evaluates the angular separation of candidates in the normalized objective space [19, 20], and clustering- and knee-point-driven variants extend it to irregular and degenerated fronts [20–22]. Such mechanisms identify directionally novel solutions well, but they rely on a fixed niche size or a fixed diversity weight and can overemphasize peripheral solutions when convergence is poor.

A common assumption underlies these families: the selection pressure is a constant of the algorithm. The population, however, is not stationary—convergence, distribution and directional diversity change substantially across generations—so a fixed pressure cannot respond to them. What is needed is a mechanism that perceives the population state, converts this perception into a bounded and smoothed pressure, and applies it inside a structured two-stage niching procedure.

Accordingly, this paper proposes DES-NSGA-II, a dynamic environmental-selection algorithm developed within the NSGA-II framework, whose closed loop consists of state perception, pressure regulation, hierarchical selection and feedback. Two robust indicators characterize complementary aspects of the population: the first measures distributional disturbance through the interquartile range and median of the perpendicular distances in the truncation front, which reduces sensitivity to extreme values; the second measures convergence discrepancy by comparing the truncation front with the first nondominated front. Both jointly determine a bounded, temporally smoothed coefficient $\beta_t$ that regulates the influence of angular novelty in the second stage.

Environmental selection is organized as a two-stage hierarchical niching procedure. Stage I builds a convergence-oriented skeleton by selecting at most one representative per occupied reference direction, according to the minimum perpendicular distance. Stage II scores further candidates by combining normalized perpendicular distance with angular novelty relative to the skeleton, under the regulation of $\beta_t$. This separates the construction of the global skeleton from directional enrichment, so that a single criterion cannot dominate the whole truncation.

DES-NSGA-II differs from three related families, and these differences constitute its main methodological advances. Against adaptive reference-vector and reference-direction methods, which adapt the reference frame, DES-NSGA-II keeps the directions fixed and adapts the pressure applied to the truncation front; the adaptation target is the intensity of selection, not the geometry. Against

two-stage methods, whose diversity stage carries a predetermined or fixed weight, the intensity here is estimated online from two state signals and then bounded and smoothed. Against angle-niching methods, which rely on a fixed angular weight, the influence of angular novelty is modulated by a state-dependent coefficient. RVEA and NSGA-III belong to the first of these families and are not part of the empirical comparison of Section 3; the claims of this paper are therefore restricted to the nine baselines of Section 3.1, and a direct comparison with these two algorithms is left for future work.

The contributions are summarized as follows:

- A dynamic environmental-selection framework, termed DES-NSGA-II, that adapts the selection pressure to the instantaneous state of the evolving population within the NSGA-II framework.
- Two robust population-state indicators for distributional disturbance and convergence discrepancy, whose joint information is transformed into a bounded and smoothed pressure coefficient.
- A two-stage hierarchical niching strategy that fixes a convergence-oriented skeleton before rewarding directional novelty under the regulation of the adaptive pressure.

We note that several foundational works cited in this paper, such as the original definitions of NSGA-II [4], MOEA/D [8], and the IGD metric [34], were published before 2020. They are retained not as recent state-of-the-art alternatives, but as the indispensable seminal definitions and baselines for this field. To ensure a rigorous and up-to-date literature review, we have substantially expanded our reference pool to include recent publications from 2020–2025, which represent the current mainstream of adaptive reference-direction and two-stage methods.

The remainder of this paper is organized as follows. Section 2 presents DES-NSGA-II, including the problem formulation, the baseline NSGA-II environmental selection, robust state perception, adaptive pressure regulation and two-stage hierarchical niching; the literature motivating each component has been reviewed in Section 1. Section 3 reports the experimental setup, the overall performance comparison, the evolution of the adaptive pressure, the statistical tests and the ablation study. Section 4 concludes the paper and discusses limitations and future work.

## 2. The proposed DES-NSGA-II

### *2.1. Problem formulation*

A many-objective optimization problem (MaOP) can be formulated as

$$\min_{\mathbf{x}\in\Omega} \mathbf{F}(\mathbf{x}) = (f_1(\mathbf{x}), f_2(\mathbf{x}), \ldots, f_M(\mathbf{x})), \tag{2.1}$$

where $\mathbf{x}$ is the decision vector, $\Omega$ denotes the decision space, $M$ is the number of objectives, and $f_m(\mathbf{x})$ is the $m$th objective function.

For two solutions $\mathbf{x}_a$ and $\mathbf{x}_b$, $\mathbf{x}_a$ is said to dominate $\mathbf{x}_b$, denoted by $\mathbf{x}_a \prec \mathbf{x}_b$, if

$$f_m(\mathbf{x}_a) \le f_m(\mathbf{x}_b), \quad m = 1, \ldots, M, \tag{2.2}$$

and there exists at least one $m \in \{1, \ldots, M\}$ such that

$$f_m(\mathbf{x}_a) < f_m(\mathbf{x}_b). \tag{2.3}$$

The Pareto-optimal set is defined as

$$\mathrm{PS} = \{\mathbf{x} \in \Omega \mid \nexists\, \mathbf{x}' \in \Omega \text{ such that } \mathbf{x}' \prec \mathbf{x}\}, \tag{2.4}$$

and its image in the objective space constitutes the Pareto front (PF).

As $M$ increases, the proportion of mutually nondominated solutions grows rapidly, so dominance-based selection alone provides insufficient discrimination among candidates. Crowding-distance mechanisms also become less informative in high-dimensional objective spaces. DES-NSGA-II therefore retains the basic evolutionary framework of NSGA-II but replaces the last-front truncation procedure with a geometry-aware, state-driven environmental-selection mechanism. The overall framework is summarized in Figure 1, and its components are detailed in Sections 2.2–2.9.

### *2.2. Baseline NSGA-II environmental selection*

NSGA-II first performs fast nondominated sorting on the combined parent–offspring population. Let $F_t^\ell$ denote the $\ell$-th nondominated front at generation $t$. The environmental selection preserves complete fronts until the population size reaches the truncation front. Specifically, let $L$ be the smallest integer satisfying

$$\sum_{\ell=1}^{L-1} |F_t^\ell| < N, \qquad \sum_{\ell=1}^{L} |F_t^\ell| \geq N, \tag{2.5}$$

so that $F_t^L$ is the first front that cannot be fully accommodated. The candidate population is

$$\mathcal{P}_t = \bigcup_{\ell=1}^{L} F_t^\ell, \tag{2.6}$$

and the next generation is formed as

$$\mathcal{P}_{t+1} = \left(\bigcup_{\ell=1}^{L-1} F_t^\ell\right) \cup F_t^{L,\mathrm{sel}}, \tag{2.7}$$

where $F_t^{L,\mathrm{sel}} \subseteq F_t^L$ contains the solutions selected to fill the remaining $K = N - \left|\bigcup_{\ell=1}^{L-1} F_t^\ell\right|$ slots.

For conventional NSGA-II, crowding distance $CD_i$ discriminates solutions within $F_t^L$. As $M$ grows, the objective space becomes sparse and crowding distance loses discriminative ability. DES-NSGA-II therefore replaces this last-front truncation with the geometry-aware procedure described below. For notational simplicity, the truncation front is denoted by $F_t^L$ throughout; this is the same front as $F_t^p$ in the original NSGA-II notation, where $p$ is the index of the last front that cannot be fully accommodated.

### *2.3. Framework overview*

DES-NSGA-II establishes a closed-loop relationship between the population state and environmental selection. As shown in Figure 1, the procedure consists of four coupled modules:

(1) **Normalization and reference-direction association.** Candidate solutions in the truncation front are normalized and associated with the nearest reference direction, yielding a directional label $r_i$ and a perpendicular distance $d_{2,i}$.

(2) **Population-state perception.** Two robust signals, $S_{1,t}$ and $S_{2,t}$, are computed from the perpendicular distances of the truncation front and the first nondominated front.
(3) **Adaptive selection-pressure regulation.** The signals are mapped to a bounded and temporally smoothed coefficient $\beta_t \in [1, 2)$.
(4) **Two-stage hierarchical niching.** Stage I constructs a convergence-oriented skeleton; Stage II enhances directional diversity under the regulation of $\beta_t$.

As shown in Figure 1, the procedure starts from the combined population $P_t$. Fast nondominated sorting determines the truncation front $F_t^L$. Normalization and reference association produce the directional label $r_i$ and the perpendicular distance $d_{2,i}$. The perception module computes $S_{1,t}$ and $S_{2,t}$. The pressure regulator maps these signals to the bounded and smoothed coefficient $\beta_t$. Stage I constructs the convergence-oriented directional skeleton, and Stage II enhances angular novelty under the regulation of $\beta_t$. The selected population $P_{t+1}$ then feeds back into the next generation's population state. This is the closed loop from the population state to selection pressure and back to the population state. The resulting selection pressure feeds back into the next generation's population state, forming the closed loop.

Population State → Selection Pressure → Environmental Selection → Population State

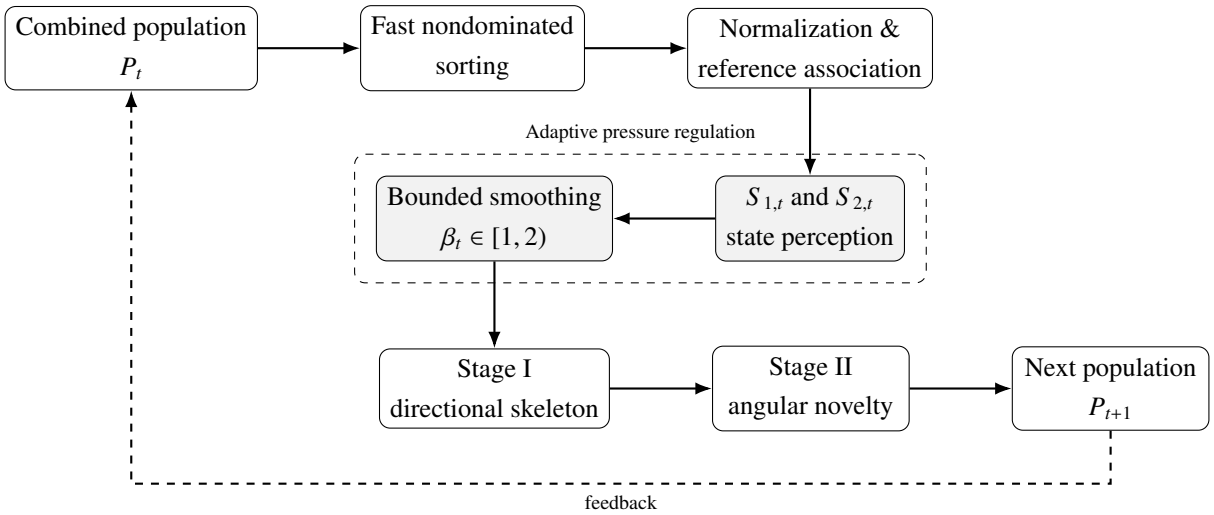


**Figure 1.** Closed-loop framework of DES-NSGA-II. The population state is perceived through two robust signals, transformed into a bounded and smoothed selection pressure, and applied within a two-stage hierarchical niching procedure.

### *2.4. Objective-space normalization and reference-direction association*

#### 2.4.1. Generation-wise objective normalization

The objective vector of solution $i$ is

$$\mathbf{f}_i = (f_{i,1}, f_{i,2}, \ldots, f_{i,M}). \tag{2.8}$$

Since objectives may have different scales, normalization is required before any geometric comparison. Within the current combined population, define

$$f_m^{\min} = \min_i f_{i,m}, \qquad f_m^{\max} = \max_i f_{i,m}. \tag{2.9}$$

The normalized objective is

$$z_{i,m} = \frac{f_{i,m} - f_m^{\min}}{f_m^{\max} - f_m^{\min} + \varepsilon}, \tag{2.10}$$

where $\varepsilon$ is a small positive constant that prevents numerical singularity when the objective range approaches zero. Intuitively, this step maps every objective to $[0, 1]$ while the additive $\varepsilon$ avoids numerical singularity when an objective has nearly zero range. The normalized vector is

$$\mathbf{z}_i = (z_{i,1}, z_{i,2}, \ldots, z_{i,M}), \tag{2.11}$$

and its unit-normalized form is

$$\bar{\mathbf{z}}_i = \frac{\mathbf{z}_i}{\|\mathbf{z}_i\|_2 + \varepsilon}. \tag{2.12}$$

The unit vector $\bar{\mathbf{z}}_i$ is used only for angular comparisons; the raw norm $\|\mathbf{z}_i\|_2$ is retained in Eq (2.16) to preserve convergence information.

### 2.4.2. Reference directions

To introduce explicit geometric information, a set of reference directions is generated in the normalized objective space:

$$\mathcal{R} = \{\mathbf{r}_1, \mathbf{r}_2, \ldots, \mathbf{r}_{N_r}\}, \qquad \|\mathbf{r}_j\|_2 = 1, \tag{2.13}$$

where $N_r$ is the number of reference directions. In the implementation, the `UniformPoint` procedure in PlatEMO [23] generates $N_r$ uniformly distributed reference points according to $N$ and $M$; each point is then normalized to unit length. The number of directions is chosen to be of the same order as the population size:

$$N_r = O(N). \tag{2.14}$$

For $M = 3, 5, 10, 15$ and $N = 100$, the values of $N_r$ are $105, 126, 110, 120$, respectively. When $N_r$ exceeds the number of candidates in the truncation front, empty directions are skipped in Stage I and the remaining slots are filled in Stage II.

For a normalized objective vector $\mathbf{z}_i$, the cosine similarity with direction $j$ is

$$\cos\phi_{ij} = \bar{\mathbf{z}}_i^{\mathrm{T}} \mathbf{r}_j. \tag{2.15}$$

The perpendicular distance is then

$$d_{2,ij} = \|\mathbf{z}_i\|_2 \sqrt{1 - \left[\mathrm{clip}\left(\bar{\mathbf{z}}_i^{\mathrm{T}} \mathbf{r}_j, -1, 1\right)\right]^2}, \tag{2.16}$$

where $\mathrm{clip}(u, -1, 1) = \min\{\max\{u, -1\}, 1\}$. The factor $\|\mathbf{z}_i\|_2$ keeps convergence information, while the angular term measures the deviation from the reference direction. Geometrically, $d_{2,ij}$ measures how far solution $i$ deviates from reference direction $j$ after the convergence magnitude $\|\mathbf{z}_i\|_2$ has been factored

out. A small $d_{2,ij}$ therefore indicates that solution $i$ is both reasonably converged and well-aligned with direction $j$. The rationale for using the perpendicular distance rather than a pure angle is that the factor $\|\mathbf{z}_i\|_2$ retains convergence information: a solution far from the origin is penalized even if its direction is well-aligned with a reference direction. Each solution is associated with the direction having the minimum perpendicular distance:

$$r_i = \arg\min_{1\le j\le N_r} d_{2,ij}, \qquad d_{2,i} = \min_{1\le j\le N_r} d_{2,ij}. \tag{2.17}$$

If several directions attain the same minimum, the one with the smallest index is chosen to ensure deterministic association. The pair $(r_i, d_{2,i})$ is the basic geometric descriptor used by the subsequent modules.

### *2.5. Robust population-state perception*

The selection pressure is regulated by the current distributional state of the population. Two complementary signals are derived from the perpendicular distances.

Let $F_t^L$ be the truncation front. Its distance set is

$$D_t^L = \left\{ d_{2,i} \mid i \in F_t^L \right\}, \tag{2.18}$$

and the corresponding set for the first nondominated front is

$$D_t^1 = \left\{ d_{2,i} \mid i \in F_t^1 \right\}. \tag{2.19}$$

These two sets describe the geometric properties of the truncation front and the current best front, respectively.

#### 2.5.1. Robust dispersion signal

The first signal measures the internal dispersion of the truncation front. Let $Q_{1,t}$ and $Q_{3,t}$ be the first and third quartiles of $D_t^L$, and let

$$\mathrm{IQR}(D_t^L) = Q_{3,t} - Q_{1,t}, \qquad \widetilde{D}_t^L = \mathrm{median}(D_t^L). \tag{2.20}$$

The robust dispersion signal is

$$S_{1,t} = \frac{\mathrm{IQR}(D_t^L)}{\widetilde{D}_t^L + \varepsilon}. \tag{2.21}$$

Unlike the coefficient of variation based on the standard deviation and mean, $S_{1,t}$ uses the interquartile range and median, and is therefore less sensitive to extreme distance values. The IQR/median ratio is used instead of the standard-deviation/mean ratio because the former is more robust to extreme perpendicular distances, which are common near the truncation front. It reflects how unevenly the truncation-front candidates are distributed across their reference directions. A large $S_{1,t}$ means that the perpendicular distances in the truncation front are widely spread, i.e., the candidates are unevenly distributed across directions; a small $S_{1,t}$ indicates a relatively uniform distribution.

2.5.2. Relative convergence-discrepancy signal

The second signal compares the truncation front with the first nondominated front. Its median is

$$\widetilde{D}_t^1 = \text{median}(D_t^1). \tag{2.22}$$

The relative convergence-discrepancy signal is

$$S_{2,t} = \max\left(\frac{\widetilde{D}_t^L}{\widetilde{D}_t^1 + \varepsilon}, 1\right), \tag{2.23}$$

so that $S_{2,t} \geq 1$. The $\max(\cdot, 1)$ operation makes $S_{2,t}$ neutral when the truncation front is geometrically no worse than the first front, and lets $S_{2,t} > 1$ indicate a relative geometric discrepancy that calls for stronger diversity enhancement. When $\widetilde{D}_t^L \leq \widetilde{D}_t^1$, the truncation front is geometrically no worse than the first front, and $S_{2,t}$ takes the neutral value one. When $\widetilde{D}_t^L > \widetilde{D}_t^1$, the truncation-front candidates deviate more from their reference directions, and $S_{2,t} > 1$. A larger $S_{2,t}$ therefore indicates a more pronounced relative geometric discrepancy between the two fronts. A large $S_{2,t}$ means that the truncation front deviates more from the reference directions than the first nondominated front does, which signals that the last-front candidates are geometrically less well-aligned and may require stronger diversity enhancement.

In summary, $S_{1,t}$ captures internal dispersion, whereas $S_{2,t}$ captures relative convergence discrepancy. The two signals provide complementary state information for the adaptive pressure regulation.

### *2.6. Adaptive selection-pressure regulation*

The two state signals are combined into a selection-pressure coefficient. To avoid an independently tuned exponent, the exponent is determined directly from $S_{2,t}$:

$$\alpha_t = \frac{1}{\ln(1 + S_{2,t}) + \varepsilon}. \tag{2.24}$$

The exponent $\alpha_t = 1/\ln(1 + S_{2,t})$ makes the sensitivity of $\beta_t^{\text{raw}}$ to $S_{2,t}$ decrease as $S_{2,t}$ grows, so the controller avoids overreacting to very large discrepancies. The raw pressure is

$$\beta_t^{\text{raw}} = S_{1,t} S_{2,t}^{\alpha_t}. \tag{2.25}$$

Since $\alpha_t > 0$, an increase in $S_{2,t}$ contributes positively to the raw pressure. At the same time, $\alpha_t$ modulates the nonlinear sensitivity of this contribution according to the observed state.

To bound the pressure, a hyperbolic tangent transformation is applied:

$$\beta_t^{\text{cur}} = 1 + \tanh\left(\beta_t^{\text{raw}}\right). \tag{2.26}$$

The hyperbolic tangent mapping is used because it is monotone and bounded; it compresses large raw pressures toward the upper bound 2 without allowing arbitrarily large selection pressure. Since $S_{1,t} \geq 0$ and $S_{2,t} \geq 1$, we have $\beta_t^{\text{raw}} \geq 0$ and therefore

$$1 \leq \beta_t^{\text{cur}} < 2. \tag{2.27}$$

The hyperbolic tangent mapping compresses large raw pressures toward the upper bound 2 while preserving monotonicity, so that the controller cannot produce arbitrarily large selection pressure even when both signals are large.

To prevent abrupt generation-to-generation changes, temporal smoothing is introduced:

$$w_t = \max\left\{w_{\min}, \frac{1}{\sqrt{t+1}}\right\}, \qquad \beta_t = w_t\beta_t^{\mathrm{cur}} + (1-w_t)\beta_{t-1}, \qquad \beta_0 = 1, \tag{2.28}$$

where $0 < w_{\min} \leq 1$ is a small lower bound introduced to prevent the smoothing weight from vanishing in later generations. The weight $w_t = 1/\sqrt{t+1}$ allows fast response in early generations and increasingly stable behavior in later generations; the lower bound $w_{\min}$ prevents the controller from becoming a frozen constant. Because $0 < w_t \leq 1$ and both $\beta_t^{\mathrm{cur}}$ and $\beta_{t-1}$ lie in $[1, 2)$, the smoothed coefficient satisfies

$$1 \leq \beta_t < 2. \tag{2.29}$$

The weight $w_t$ decreases with $t$ until it reaches the lower bound, so that early generations can respond quickly to the perceived state while later generations rely more on the smoothed history and avoid abrupt fluctuations. The lower bound also prevents the controller from degenerating into a frozen constant in the late stage. The resulting $\beta_t$ is an automatically regulated variable rather than a manually tuned parameter. It is used in Stage II to control the influence of angular novelty.

**Proposition 1.** *Assume $S_{1,t} \geq 0$, $S_{2,t} \geq 1$, $\beta_0 = 1$, and $0 < w_t \leq 1$. Then $1 \leq \beta_t < 2$ for all $t \geq 0$.*

*Proof.* Since $\beta_t^{\mathrm{raw}} \geq 0$, we have

$$\beta_t^{\mathrm{cur}} = 1 + \tanh(\beta_t^{\mathrm{raw}}) \in [1, 2).$$

The smoothed value $\beta_t$ is a convex combination of $\beta_t^{\mathrm{cur}}$ and $\beta_{t-1}$. By induction, both terms lie in $[1, 2)$, so the convex combination also lies in $[1, 2)$. □

### *2.7. Two-stage environmental selection*

After nondominated sorting and reference-direction association, DES-NSGA-II retains all complete fronts preceding $F_t^L$ and performs specialized selection only on $F_t^L$. The number of solutions to be selected from $F_t^L$ is

$$K = N - \left|\bigcup_{\ell=1}^{L-1} F_t^{\ell}\right|. \tag{2.30}$$

Let

$$C_{j,t} = \left\{i \in F_t^L \mid r_i = j\right\} \tag{2.31}$$

denote the candidates associated with reference direction $j$, and let $C_{j,t}^{\mathrm{rem}}$ denote the subset not yet selected.

#### 2.7.1. Stage I: Directional representative selection

Stage I constructs a global geometric skeleton by selecting at most one representative from each available reference direction. For each direction with $C_{j,t}^{\mathrm{rem}} \neq \emptyset$, the representative is

$$i_j^* = \arg\min_{i \in C_{j,t}^{\mathrm{rem}}} d_{2,i}. \tag{2.32}$$

The selected solution is removed from $C_{j,t}^{\text{rem}}$, and the occupancy $n_{j,t}$ of direction $j$ is increased by one. Stage I emphasizes directional convergence and ensures that the skeleton covers as many available directions as possible. If $K$ solutions are reached during this stage, the procedure terminates without entering Stage II.

#### 2.7.2. Stage II: Adaptive direction prioritization

If additional solutions are required, Stage II fills the remaining slots. Unlike Stage I, Stage II does not impose a one-solution-per-direction constraint, so a direction may contribute multiple solutions as long as unselected candidates remain. The set of available directions is

$$\mathcal{J}_t^{\text{avail}} = \left\{ j \mid \left| C_{j,t}^{\text{rem}} \right| > 0 \right\}. \tag{2.33}$$

To characterize the potential contribution of each direction, define

$$A_{j,t} = \frac{\left| C_{j,t}^{\text{rem}} \right|}{n_{j,t} + 1}, \tag{2.34}$$

which increases when a direction has many remaining candidates relative to its current occupancy. The direction-priority score is

$$G_{j,t} = n_{j,t} - 2A_{j,t}. \tag{2.35}$$

The direction processed at each iteration is

$$j^* = \arg \min_{j \in \mathcal{J}_t^{\text{avail}}} G_{j,t}. \tag{2.36}$$

Thus, directions with low occupancy and sufficient remaining candidates receive higher priority. The factor 2 in Eq (2.35) is a deterministic prioritization constant rather than an additional tuned parameter; its sensitivity is examined in Section 3.5. Once a direction is exhausted, it is removed from $\mathcal{J}_t^{\text{avail}}$. The process continues until $K$ solutions have been selected or no candidate remains.

#### 2.7.3. Angular novelty evaluation

Within the selected direction $j^*$, candidates are evaluated by convergence and angular novelty. Let $\mathcal{S}_t$ be the set of solutions selected so far. For candidate $i$ and selected solution $k$, the angular separation is

$$\theta_{ik} = \arccos\left[\text{clip}\left(\bar{\mathbf{z}}_i^{\mathrm{T}} \bar{\mathbf{z}}_k, -1, 1\right)\right], \tag{2.37}$$

and the minimum angular distance to the selected set is

$$\theta_i = \min_{k \in \mathcal{S}_t} \theta_{ik}. \tag{2.38}$$

A larger $\theta_i$ indicates greater directional novelty.

When $\mathcal{S}_t \neq \emptyset$, the perpendicular distances of the remaining candidates in direction $j^*$ are normalized as

$$\bar{d}_{2,i} = \frac{d_{2,i} - d_2^{\min}}{d_2^{\max} - d_2^{\min} + \varepsilon}, \tag{2.39}$$

where $d_2^{\min}$ and $d_2^{\max}$ are the minimum and maximum $d_2$ values among these candidates. The angular novelty is normalized as

$$\overline{\theta}_i = \frac{\theta_i}{\theta^{\max} + \varepsilon}, \qquad \theta^{\max} = \max_i \theta_i. \tag{2.40}$$

The candidate score is

$$\mathrm{Score}_{i,t} = \overline{d}_{2,i} + \beta_t \overline{\theta}_i, \tag{2.41}$$

and the candidate with the smallest score is selected:

$$i^* = \arg\min_i \mathrm{Score}_{i,t}. \tag{2.42}$$

The first term favors convergence, whereas the second term rewards angular novelty. Because $\beta_t$ is state-dependent, the relative influence of angular novelty changes adaptively across generations. If $\mathcal{S}_t = \emptyset$, no angular comparison is possible, and the candidate with the smallest $d_{2,i}$ is selected to provide a convergence-oriented initialization.

### *2.8. Overall selection procedure*

The complete environmental-selection procedure is summarized in Algorithm 1 and illustrated in Figure 1. First, fast nondominated sorting is performed on the combined population, and all complete fronts preceding $F_t^L$ are retained. The candidates in $F_t^L$ are normalized and associated with reference directions. Second, $S_{1,t}$ and $S_{2,t}$ are computed from $D_t^L$ and $D_t^1$, and the bounded, smoothed pressure $\beta_t$ is obtained through

$$S_{1,t}, S_{2,t} \longrightarrow \alpha_t \longrightarrow \beta_t^{\mathrm{raw}} \longrightarrow \beta_t^{\mathrm{cur}} \longrightarrow \beta_t. \tag{2.43}$$

Third, Stage I selects at most one representative per available direction. Finally, if additional solutions are needed, Stage II prioritizes directions by $G_{j,t}$ and selects candidates by Eq (2.41). The procedure forms the closed loop of Eq (2.44) and does not introduce new hyperparameters that require manual tuning.

$$\text{Population State} \rightarrow \text{Selection Pressure} \rightarrow \text{Environmental Selection} \rightarrow \text{Population State} \tag{2.44}$$

### *2.9. Computational complexity*

Let $N$, $M$, and $N_r$ denote the population size, the number of objectives, and the number of reference directions, respectively. Fast nondominated sorting costs $O(MN^2)$. Reference-direction association costs $O(MNN_r)$, which becomes $O(MN^2)$ when $N_r = O(N)$. Population-state perception and candidate sorting cost at most $O(N \log N)$. Stage I costs $O(N)$, and Stage II costs at most $O(MN^2)$ because $O(N)$ candidates are compared with up to $O(N)$ selected solutions. The additional complexity is therefore

$$O(MNN_r) + O(MN^2) + O(N \log N) = O(MN^2), \tag{2.45}$$

and the overall worst-case complexity of DES-NSGA-II remains

$$O(MN^2). \tag{2.46}$$

Thus, the proposed environmental selection does not increase the asymptotic complexity of the underlying NSGA-II framework.

**Algorithm 1** Environmental selection of DES-NSGA-II

**Require:** $P_t$, $N$, $\mathcal{R} = \{\mathbf{r}_j\}_{j=1}^{N_r}$
**Ensure:** $P_{t+1}$
Fast nondominated sorting on $P_t$; find truncation front $F_t^L$ by Eq (2.5)
$P_{t+1} \leftarrow \bigcup_{\ell=1}^{L-1} F_t^\ell$; $K \leftarrow N - |P_{t+1}|$
**if** $K = 0$ **then**
    **return** $P_{t+1}$
**end if**
Normalize $F_t^L$ by Eq (2.10); associate each $i$ with $(r_i, d_{2,i})$ by Eq (2.17); build clusters $C_{j,t}$
Compute $S_{1,t}$, $S_{2,t}$, and $\beta_t$ by Eqs (2.21)–(2.28)
**Stage I: directional skeleton**
**for** each $j$ with $C_{j,t}^{\mathrm{rem}} \neq \emptyset$ **do**
    $i_j^* \leftarrow \arg\min_{i \in C_{j,t}^{\mathrm{rem}}} d_{2,i}$; update $P_{t+1}$, $C_{j,t}^{\mathrm{rem}}$, $n_{j,t}$
    **if** $|P_{t+1}| = N$ **then**
        **return** $P_{t+1}$
    **end if**
**end for**
**Stage II: adaptive direction prioritization**
**while** $|P_{t+1}| < N$ and $\mathcal{J}_t^{\mathrm{avail}} \neq \emptyset$ **do**
    $j^* \leftarrow \arg\min_{j \in \mathcal{J}_t^{\mathrm{avail}}} G_{j,t}$ by Eqs (2.34)–(2.36)
    **if** $\mathcal{S}_t = \emptyset$ **then**
        $i^* \leftarrow \arg\min_{i \in C_{j^*,t}^{\mathrm{rem}}} d_{2,i}$
    **else**
        $i^* \leftarrow \arg\min_i \mathrm{Score}_{i,t}$ by Eqs (2.37)–(2.42)
    **end if**
    Update $P_{t+1}$, $C_{j^*,t}^{\mathrm{rem}}$, $n_{j^*,t}$; remove $j^*$ if exhausted
**end while**
**return** $P_{t+1}$

## 3. Experimental results and discussion

### *3.1. Experimental setup*

To comprehensively evaluate the performance of DES-NSGA-II, it is compared with nine representative multi-objective evolutionary algorithms, including CMOEA-CD [22], IMC-MOEAD [24], LERD [25], NRVMOEA [26], FDV [27], HEA [28], LMPFE [29], DGEA [30], and NSGAII-ARSBX [31]. All experiments are conducted on the PlatEMO platform [23] under a unified experimental environment. RVEA and NSGA-III are not included in this comparison. The purpose of the present study is to isolate the effect of a state-driven selection pressure inside a decomposition-free, dominance-based framework, and the nine baselines above were selected to cover the decomposition-, indicator-, direction- and model-based families under that constraint. The methodological relation to the two reference-vector families is discussed in Section 1, and no empirical claim is made about them in this paper. IM-MOEA/D is cited from its conference

proceedings, since that is the only published description of this decomposition-based variant; the inverse-modeling scheme it builds on is that of Cheng et al. [7].

For a fair comparison, all algorithms use the same population size of $N = 100$ whenever applicable. DES-NSGA-II and the corresponding evolutionary algorithms employ simulated binary crossover (SBX) and polynomial mutation (PM) [32, 33]. The genetic-operator parameters are set to

$$p_c = 0.8, \qquad \eta_c = 20, \qquad p_m = 0.1, \qquad \eta_m = 20. \tag{3.1}$$

Algorithm-specific parameters are configured according to the settings recommended in their respective original publications. The maximum number of function evaluations is adopted as the termination criterion and is set to

$$\text{maxFE} = M \times 10^4, \tag{3.2}$$

where $M$ denotes the number of objectives.

Statistical analysis: Each algorithm is independently executed 30 times on every test instance. Two indicators are recorded for every run. IGD [34] measures the average distance from each reference point to its nearest solution and therefore mixes convergence and distribution into a single value. IGD$^+$ [35] replaces the Euclidean distance of IGD by a distance that is dominated-aware, so that a solution is not penalized for being close to the reference front but dominated by it; the definition originates in conference proceedings, and its convergence and diversity behavior was further analyzed in the journal survey of [15]. Both indicators are computed with the reference sets described below, and the IGD$^+$ implementation is the PlatEMO routine [23]. For each test instance and each performance indicator, the $r$-th run ($r = 1, \ldots, 30$) of DES-NSGA-II and that of each competitor are performed with the same random seed, yielding 30 paired observations per instance. The two-sided Wilcoxon signed-rank test [36] is then applied to these 30 pairs at $\alpha = 0.05$; the null hypothesis is that the median paired difference is zero. In the result tables, "+" indicates that the competitor performs significantly better than DES-NSGA-II, "−" indicates that DES-NSGA-II performs significantly better, and "=" indicates no statistically significant difference.

For the Friedman test, each test instance is treated as one block, giving $N = 84$ blocks in total (DTLZ: $7 \times 4$, WFG: $7 \times 4$, MaF: $7 \times 4$). Within each block, the ten algorithms are ranked according to their mean IGD or IGD$^+$ over 30 runs. The Friedman statistic is computed from these 84 blocks, and Kendall's $W$ is reported as the effect size. The Holm post-hoc procedure is applied to the nine average-rank comparisons between DES-NSGA-II and each competitor. In addition, per-instance two-sided Wilcoxon signed-rank tests at $\alpha = 0.05$ are used to count wins/ties/losses (W/T/L).

A three-step analysis, namely convergence, stability, and significance testing, follows the convergence–stability–significance reporting convention used in recent forecasting studies [37, 38]: the convergence behavior is examined through the mean indicator values, run-to-run stability is assessed through the boxplots in Figure 2, and the Wilcoxon and Friedman tests are finally applied to establish statistical significance.

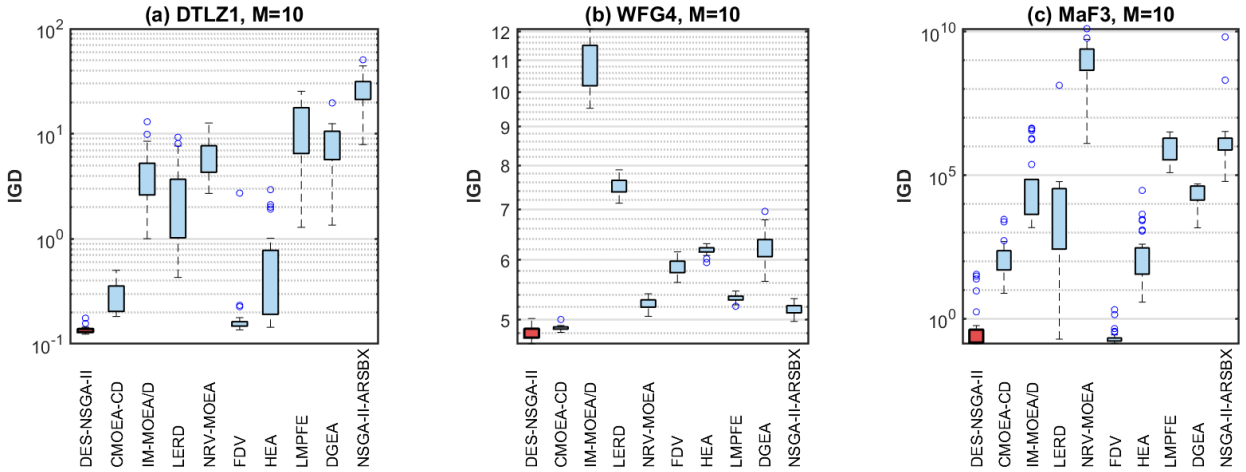


**Figure 2.** Run-to-run convergence stability on representative instances. Boxplots summarize the IGD values of 30 independent runs on (a) DTLZ1 with $M = 10$, (b) WFG4 with $M = 10$, and (c) MaF3 with $M = 10$. The central line, box, and whiskers denote the median, interquartile range (25th–75th percentiles), and 1.5×IQR, respectively; points denote outliers. Lower IGD is better. The $y$-axis is shown on a logarithmic scale.

To further assess the overall performance differences among the compared algorithms, the Friedman test [36] is employed separately for IGD and IGD$^+$ over the complete set of test instances. For each test instance, the algorithms are ranked according to their mean indicator values over 30 runs (rank 1 denotes the best), and the average ranks are then computed for the DTLZ, WFG, and MaF suites as well as over all instances. The Holm post-hoc procedure is used to control the family-wise error rate for the nine pairwise comparisons between DES-NSGA-II and each competitor. A pairwise comparison is declared significant when the Holm-adjusted $p$-value is less than 0.05. The Wilcoxon and Friedman analyses provide complementary statistical evidence for evaluating the pairwise and overall performance of DES-NSGA-II.

For reproducibility, the IGD and IGD$^+$ reference sets were generated by the default PlatEMO routine and kept identical for all algorithms. All experiments were run on PlatEMO under MATLAB. For $M = 3, 5, 10, 15$ and $N = 100$, the reference directions were generated by the `UniformPoint` procedure, yielding $N_r = 105, 126, 110, 120$. The LinearDecay baseline uses $\beta_t = \max\{\beta_{\min}, \beta_0 - (\beta_0 - \beta_{\min})t/T\}$ with $\beta_0 = 1.5$, $\beta_{\min} = 1.0$, and $T = \text{maxFE}$.

### *3.2. Overall performance comparison*

The main IGD and IGD$^+$ comparisons on the DTLZ, WFG and MaF suites are summarized in Tables 1–6. On the 28 DTLZ instances, DES-NSGA-II wins 22, ties 1 and loses 5 against CMOEA-CD in terms of IGD, and it obtains the best average rank on all three suites, namely 1.607, 1.821 and 2.357 (Table 7).

**Table 1.** IGD values on DTLZ test problems.

| Problem | $M$ | IGD | | | | | | | | | |
|---|---|---|---|---|---|---|---|---|---|---|---|
| | | CMOEA-CD | IMC-MOEAD | LERD | NRVMOEA | FDV | HEA | LMPFE | DGEA | NSGAII-ARSBX | DES-NSGA-II |
| DTLZ1 | 3 | **2.0329e-2** | 3.9251e+0 | 7.5285e-1 | 9.5896e-2 | 2.1860e-2 | 1.0666e-1 | 1.6791e-1 | 1.2838e+1 | 1.8650e+0 | **2.3972e-2** |
| | | **(3.11e-4)+** | (1.51e+0) - | (1.41e+0) - | (1.07e-1) - | (1.64e-3)+ | (1.57e-1) - | (1.77e-1) - | (7.63e+0) - | (1.93e+0) - | (1.36e-3) |
| | 5 | 3.3277e-1 | 3.8856e+0 | 1.8359e+0 | 6.7228e-1 | 7.9835e-2 | 2.6933e-1 | 7.8467e-1 | 9.6537e+0 | 1.6137e+1 | **6.7849e-2** |
| | | (1.03e+0) - | (1.74e+0) - | (2.14e+0) - | (4.31e-1) - | (1.29e-2) - | (2.65e-1) - | (4.65e-1) - | (8.14e+0) - | (5.86e+0) - | **(1.82e-3)** |
| | 10 | 2.7585e-1 | 4.3443e+0 | 2.8607e+0 | 6.3350e+0 | 2.4550e-1 | 6.3658e-1 | 1.2163e+1 | 7.8648e+0 | 2.6509e+1 | **1.3560e-1** |
| | | (1.04e-1) - | (2.76e+0) - | (2.39e+0) - | (2.63e+0) - | (4.69e-1) - | (7.05e-1) - | (7.00e+0) - | (3.98e+0) - | (9.43e+0) - | **(1.04e-2)** |
| | 15 | 2.8345e-1 | 8.6146e+0 | 7.4471e+0 | 6.6101e+0 | 2.1378e-1 | 6.1029e-1 | 7.2050e+0 | 6.2122e+0 | 3.8170e+0 | **1.7218e-1** |
| | | (6.77e-2) - | (3.59e+0) - | (7.31e+0) - | (3.37e+0) - | (4.98e-2) - | (6.63e-1) - | (3.03e+0) - | (3.90e+0) - | (2.28e+0) - | **(1.38e-2)** |
| DTLZ2 | 3 | 5.5887e-2 | 1.1940e-1 | 6.5729e-2 | 6.3240e-2 | 5.7677e-2 | 5.6240e-2 | 5.6263e-2 | 6.0276e-2 | 7.0265e-2 | **4.8679e-2** |
| | | (4.80e-4) - | (9.61e-3) - | (1.80e-3) - | (1.35e-3) - | (9.88e-4) - | (6.74e-4) - | (4.29e-4) - | (1.32e-2) - | (2.04e-3) - | **(6.53e-4)** |
| | 5 | 2.2735e-1 | 4.3722e-1 | 4.0752e-1 | 2.1679e-1 | 2.6038e-1 | 2.1607e-1 | 2.1189e-1 | 3.3414e-1 | 5.3046e-1 | **1.9259e-1** |
| | | (3.23e-3) - | (3.18e-2) - | (3.69e-2) - | (1.24e-3) - | (7.61e-3) - | (1.22e-3) - | (1.71e-3) - | (2.53e-2) - | (1.16e-1) - | **(1.81e-3)** |
| | 10 | 6.1590e-1 | 9.8826e-1 | 9.1007e-1 | 4.8836e-1 | 7.5922e-1 | 5.4329e-1 | 4.9987e-1 | 8.1976e-1 | 1.4171e+0 | **4.5619e-1** |
| | | (2.12e-2) - | (7.24e-2) - | (4.71e-2) - | (6.03e-3) - | (8.26e-2) - | (4.56e-3) - | (2.50e-2) - | (6.44e-2) - | (1.42e-1) - | **(4.11e-3)** |
| | 15 | 8.0800e-1 | 1.1604e+0 | 1.0772e+0 | 5.9844e-1 | 1.1310e+0 | 7.4879e-1 | 6.2725e-1 | 1.1432e+0 | 2.4684e+0 | **5.7921e-1** |
| | | (5.35e-2) - | (3.58e-2) - | (6.65e-2) - | (1.05e-2) - | (8.59e-2) - | (1.43e-2) - | (3.30e-2) - | (5.05e-2) - | (2.45e-1) - | **(5.77e-3)** |
| DTLZ3 | 3 | 2.6223e-1 | 6.5102e+1 | 3.7121e+1 | 7.5190e+0 | **5.9964e-2** | 6.8728e+0 | 7.4276e+0 | 8.6532e+1 | 8.0823e+1 | 3.2502e-1 |
| | | (4.71e-1)+ | (1.27e+1) - | (3.58e+1) - | (4.79e+0) - | **(3.31e-3)+** | (5.12e+0) - | (4.99e+0) - | (4.65e+1) - | (6.47e+1) - | (4.18e-1) |
| | 5 | 8.3527e-1 | 7.6237e+1 | 2.9416e+1 | 2.9632e+1 | 5.1892e-1 | 4.7377e+0 | 3.2857e+1 | 7.6557e+1 | 1.5298e+2 | **3.2482e-1** |
| | | (8.20e-1) - | (1.99e+1) - | (2.85e+1) - | (1.03e+1) - | (2.25e-1) - | (2.94e+0) - | (1.15e+1) - | (4.00e+1) - | (2.63e+1) - | **(2.69e-1)** |
| | 10 | 2.8281e+0 | 7.7268e+1 | 6.3704e+1 | 1.0586e+2 | 1.0789e+0 | 6.8576e+0 | 2.4683e+2 | 8.6859e+1 | 6.7654e+2 | **5.0119e-1** |
| | | (1.93e+0) - | (1.48e+1) - | (4.38e+1) - | (2.17e+1) - | (3.01e-1) - | (4.33e+0) - | (1.20e+2) - | (4.72e+1) - | (2.65e+2) - | **(1.16e-2)** |
| | 15 | 3.5449e+0 | 6.6714e+1 | 8.6103e+1 | 1.4283e+2 | 1.1910e+0 | 8.9145e+0 | 7.2410e+1 | 5.8415e+1 | 7.6697e+2 | **6.4731e-1** |
| | | (3.37e+0) - | (1.80e+1) - | (6.08e+1) - | (2.99e+1) - | (3.69e-2) - | (7.48e+0) - | (5.17e+1) - | (4.40e+1) - | (4.31e+2) - | **(4.83e-2)** |
| DTLZ4 | 3 | **5.5937e-2** | 2.6360e-1 | 4.7758e-1 | 2.5338e-1 | 2.1382e-1 | 3.3935e-1 | 1.9677e-1 | 2.4600e-1 | 6.8691e-2 | 1.8045e-1 |
| | | **(7.69e-4)+** | (1.51e-1) - | (5.61e-1) - | (2.61e-1) - | (1.63e-1) - | (3.11e-1) - | (2.73e-1) - | (1.48e-1) - | (2.35e-3) + | (2.21e-1) |
| | 5 | 2.2201e-1 | 6.0038e-1 | 4.1491e-1 | 2.4198e-1 | 4.3514e-1 | 5.4041e-1 | 2.4272e-1 | 4.9777e-1 | 2.9342e-1 | **1.9432e-1** |
| | | (3.02e-3) - | (5.20e-2) - | (4.76e-2) - | (8.43e-2) - | (4.41e-2) - | (2.11e-1) - | (6.20e-2) - | (6.46e-2) - | (1.45e-2) - | **(1.87e-3)** |
| | 10 | 5.9702e-1 | 1.1561e+0 | 7.1926e-1 | 4.9415e-1 | 6.5147e-1 | 6.8280e-1 | 7.5657e-1 | 7.8815e-1 | 1.4695e+0 | **4.6159e-1** |
| | | (1.36e-2) - | (4.93e-2) - | (2.54e-2) - | (2.40e-3) - | (2.69e-2) - | (7.38e-2) - | (9.91e-2) - | (3.89e-2) - | (1.50e-1) - | **(5.43e-3)** |
| | 15 | 7.6206e-1 | 1.2516e+0 | 1.0336e+0 | 6.3839e-1 | 7.8915e-1 | 9.3618e-1 | 7.1947e-1 | 9.1219e-1 | 2.2975e+0 | **5.7531e-1** |
| | | (2.58e-2) - | (5.11e-2) - | (6.17e-2) - | (2.93e-3) - | (3.11e-2) - | (6.86e-2) - | (1.46e-1) - | (3.50e-2) - | (1.29e-1) - | **(4.66e-3)** |
| DTLZ5 | 3 | 6.6154e-3 | 3.2554e-2 | 2.3898e-2 | 5.5369e-3 | 3.3475e-2 | 3.3963e-2 | 4.9394e-3 | 5.7549e-2 | 6.1988e-3 | **5.8751e-3** |
| | | (6.23e-4) - | (6.15e-3) - | (6.45e-4) - | (2.80e-4)+ | (1.49e-3) - | (2.30e-3) - | (1.77e-4)+ | (1.13e-2) - | (3.61e-4) - | **(3.63e-4)** |
| | 5 | 2.5316e-1 | 7.6329e-2 | 1.5112e-1 | 1.0094e-1 | 1.1666e-1 | 1.2214e-1 | 1.7639e-1 | 1.4489e-1 | 1.5792e-1 | **5.1205e-2** |
| | | (4.53e-2) - | (1.22e-2) - | (3.02e-2) - | (2.38e-2) - | (2.66e-2) - | (3.89e-2) - | (4.10e-2) - | (3.49e-2) - | (5.75e-2) - | **(1.38e-2)** |
| | 10 | 5.6184e-1 | 3.5537e-1 | 3.0170e-1 | 1.9933e-1 | 5.7857e-1 | 2.7535e-1 | 3.8277e-1 | 1.5002e-1 | 5.0363e-1 | **1.4517e-1** |
| | | (1.25e-1) - | (1.05e-1) - | (5.86e-2) - | (3.08e-2) - | (2.53e-1) - | (6.48e-2) - | (1.14e-1) - | (2.63e-2) = | (1.42e-1) - | **(3.95e-2)** |
| | 15 | 5.0430e-1 | 3.9708e-1 | 3.4675e-1 | 2.2063e-1 | 7.2612e-1 | 3.6838e-1 | 1.7167e-1 | 3.7668e-1 | 4.5482e-1 | **1.5340e-1** |
| | | (1.67e-1) - | (6.67e-2) - | (6.13e-2) - | (3.54e-2) - | (3.29e-2) - | (5.53e-2) - | (1.07e-1) - | (1.42e-1) - | (1.42e-1) - | **(4.91e-2)** |
| DTLZ6 | 3 | **4.1901e-3** | 4.6431e+0 | 2.4152e-2 | 5.7345e-3 | 1.5775e+0 | 4.5710e-2 | 4.6213e-3 | 1.2081e+0 | 5.7684e-3 | 5.6832e-3 |
| | | **(3.73e-5)+** | (1.76e-1) - | (4.07e-4) - | (9.62e-4) = | (9.48e-1) - | (6.01e-3) - | (3.60e-4)+ | (1.13e+0) - | (2.44e-4) = | (4.60e-4) |
| | 5 | 1.8654e-1 | 4.3522e+0 | 1.4067e-1 | 3.3138e-1 | 2.7967e+0 | 4.7916e-1 | 1.9835e+0 | 2.0881e+0 | 3.2547e+0 | **1.1051e-1** |
| | | (6.39e-2) - | (2.12e-1) - | (7.65e-2) - | (2.57e-1) - | (1.05e+0) - | (2.24e-1) - | (7.25e-1) - | (1.07e+0) - | (1.01e+0) - | **(2.54e-2)** |
| | 10 | 5.6591e-1 | 4.2043e+0 | 3.5630e-1 | 1.2165e+0 | 3.3537e+0 | 1.6524e+0 | 4.6822e+0 | 1.7367e+0 | 5.5412e+0 | **1.9553e-1** |
| | | (2.85e-1) - | (2.82e-1) - | (1.68e-1) - | (4.77e-1) - | (1.08e+0) - | (1.12e+0) - | (9.15e-1) - | (8.99e-1) - | (1.07e+0) - | **(6.59e-2)** |
| | 15 | 7.4209e-1 | 6.9582e+0 | 4.2718e-1 | 3.9933e-1 | 1.8622e+0 | 8.3017e-1 | 1.2680e+0 | 9.9196e-1 | 3.2605e+0 | **2.2586e-1** |
| | | (3.39e-16) - | (5.20e-1) - | (8.51e-2) - | (9.15e-2) - | (1.10e+0) - | (3.89e-1) - | (1.40e+0) - | (5.19e-1) - | (1.18e+0) - | **(8.04e-2)** |
| DTLZ7 | 3 | **6.0640e-2** | 2.2662e-1 | 7.5931e-1 | 9.4745e-2 | 7.0767e-1 | 2.9347e-1 | 1.9123e-1 | 1.9589e+0 | 8.3257e-2 | 7.7722e-2 |
| | | **(1.25e-3)+** | (5.23e-2) - | (1.52e-1) - | (9.05e-2) - | (1.85e-1) - | (3.56e-1) - | (2.08e-1) - | (1.01e+0) - | (3.56e-3) - | (7.26e-2) |
| | 5 | 3.6719e-1 | 8.7663e-1 | 1.4183e+0 | 3.1978e-1 | 1.1670e+0 | 1.4112e+0 | 1.2833e+0 | 1.3877e+0 | 1.2053e+0 | **3.0469e-1** |
| | | (1.25e-2) - | (1.66e-1) - | (4.06e-1) - | (7.02e-2) - | (2.32e-1) - | (8.74e-1) - | (4.48e-1) - | (3.92e-1) - | (1.80e-1) - | **(1.13e-2)** |
| | 10 | 1.6538e+0 | 2.1126e+1 | 6.4379e+0 | 1.6312e+0 | 1.8897e+0 | 5.5218e+0 | 1.5052e+1 | 2.0674e+0 | 3.1786e+0 | **1.0958e+0** |
| | | (1.35e-1) - | (4.09e+0) - | (1.25e+0) - | (4.05e-1) - | (2.50e-1) - | (1.25e+0) - | (3.94e+0) - | (4.64e-1) - | (1.70e+0) - | **(1.29e-1)** |
| | 15 | 4.6935e+0 | 2.5883e+1 | 1.5280e+1 | **1.5467e+0** | 3.2323e+0 | 1.2067e+1 | 5.6206e+0 | 3.3703e+0 | 3.1627e+0 | 4.8510e+0 |
| | | (9.58e-1) = | (5.41e+0) - | (4.98e+0) - | **(2.99e-2)+** | (5.77e-1)+ | (2.93e-4) - | (8.03e+0) - | (9.68e-1)+ | (6.90e-1)+ | (1.11e+0) |
| +/ − / = | | 5/22/1 | 0/28/0 | 0/27/1 | 2/25/1 | 3/25/0 | 0/28/0 | 2/26/0 | 1/26/1 | 2/25/1 | |

**Table 2.** IGD values on WFG test problems.

| Problem | M | IGD | | | | | | | | | |
|---|---|---|---|---|---|---|---|---|---|---|---|
| | | CMOEA-CD | IMC-MOEAD | LERD | NRVMOEA | FDV | HEA | LMPFE | DGEA | NSGAII-ARSBX | DES-NSGA-II |
| WFG1 | 3 | 3.4451e-1 | 1.4462e+0 | 1.2777e+0 | 2.1707e-1 | 1.5548e+0 | 4.2066e-1 | **1.8525e-1** | 1.6065e+0 | 8.6227e-1 | 2.1585e-1 |
| | | (7.41e-2) - | (6.55e-2) - | (1.71e-1) - | (2.22e-2) = | (3.31e-1) - | (7.55e-2) - | **(1.99e-2)+** | (6.44e-2) - | (9.31e-2) - | (2.51e-2) |
| | 5 | 7.7734e-1 | 2.1269e+0 | 2.0179e+0 | 1.2657e+0 | 1.9990e+0 | 9.1879e-1 | 1.1051e+0 | 2.0759e+0 | 1.0325e+0 | **4.5046e-1** |
| | | (7.92e-2) - | (1.30e-1) - | (1.95e-1) - | (1.19e-1) - | (2.24e-1) - | (1.80e-1) - | (1.38e-1) - | (9.71e-2) - | (7.72e-2) - | **(1.28e-2)** |
| | 10 | 1.5318e+0 | 3.0564e+0 | 3.0952e+0 | **1.1432e+0** | 2.5790e+0 | 1.7833e+0 | 1.5540e+0 | 3.0799e+0 | 2.1317e+0 | 1.1640e+0 |
| | | (9.32e-2) - | (1.76e-1) - | (1.59e-1) - | **(2.61e-2)+** | (1.52e-1) - | (1.93e-1) - | (6.71e-2) - | (1.20e-1) - | (8.29e-2) - | (3.22e-2) |
| | 15 | **1.2851e+0** | 4.0676e+0 | 4.2028e+0 | 3.0964e+0 | 3.3249e+0 | 3.1725e+0 | 2.6412e+0 | 4.0454e+0 | 3.5784e+0 | 1.5919e+0 |
| | | **(1.66e-1)** + | (1.82e-1) - | (2.27e-1) - | (1.80e-1) - | (2.32e-1) - | (4.25e-1) - | (2.19e-1) - | (1.68e-1) - | (2.16e-1) - | (2.19e-2) |
| WFG2 | 3 | 1.8028e-1 | 2.8331e-1 | 3.1405e-1 | 1.7420e-1 | 2.0675e-1 | 1.6646e-1 | 1.8306e-1 | 3.5588e-1 | 2.2325e-1 | **1.4582e-1** |
| | | (4.59e-3) - | (1.03e-2) - | (1.71e-2) - | (5.13e-3) - | (9.87e-3) - | (4.23e-3) - | (7.45e-3) - | (5.76e-2) - | (1.50e-2) - | **(4.34e-3)** |
| | 5 | 6.3483e-1 | 8.7841e-1 | 8.8511e-1 | 5.9656e-1 | 5.7742e-1 | 5.0077e-1 | 6.6965e-1 | 7.1684e-1 | 8.9755e-1 | **4.5094e-1** |
| | | (2.33e-2) - | (1.30e-1) - | (7.14e-2) - | (1.89e-2) - | (2.63e-2) - | (1.31e-2) - | (2.95e-2) - | (5.07e-2) - | (6.77e-2) - | **(6.79e-3)** |
| | 10 | 1.9306e+0 | 3.8594e+0 | 2.4527e+0 | **1.2209e+0** | 1.5798e+0 | 1.5283e+0 | 1.8691e+0 | 1.6946e+0 | 1.8765e+0 | 1.2986e+0 |
| | | (1.23e-1) - | (1.04e+0) - | (5.82e-1) - | **(2.89e-2) =** | (6.30e-2) - | (5.39e-1) - | (1.27e-1) - | (1.53e-1) - | (1.37e-1) - | (2.24e-1) |
| | 15 | 2.6808e+0 | 8.6235e+0 | 4.9582e+0 | **1.8632e+0** | 2.2481e+0 | 3.5452e+0 | 1.9588e+0 | 3.1231e+0 | 2.5883e+0 | 3.0383e+0 |
| | | (2.01e-1)+ | (2.56e+0) - | (9.08e-1) - | **(9.98e-2)+** | (6.88e-2)+ | (1.32e+0) = | (1.16e-1)+ | (3.74e-1) = | (3.18e-1)+ | (4.95e-1) |
| WFG3 | 3 | 1.5884e-1 | 1.8483e-1 | 1.6271e-1 | 7.9756e-2 | 2.6257e-1 | **7.6789e-2** | 1.2221e-1 | 4.0219e-1 | 1.2496e-1 | 9.9766e-2 |
| | | (1.59e-2) - | (1.38e-2) - | (3.47e-2) - | (6.81e-3)+ | (3.32e-2) - | **(8.36e-3)+** | (1.08e-2) - | (3.90e-2) - | (1.50e-2) - | (8.48e-3) |
| | 5 | 8.5221e-1 | **3.6597e-1** | 7.6211e-1 | 6.7962e-1 | 1.5900e+0 | 5.0023e-1 | 7.7163e-1 | 1.3169e+0 | 5.0740e-1 | 5.0318e-1 |
| | | (1.01e-1) - | **(4.92e-2)+** | (1.13e-1) - | (5.88e-2) - | (4.96e-1) - | (6.59e-2) = | (9.25e-2) - | (1.64e-1) - | (8.80e-2) = | (7.89e-2) |
| | 10 | 3.0579e+0 | 1.2469e+0 | 2.6352e+0 | 1.7148e+0 | 6.8708e+0 | 1.5170e+0 | 3.2624e+0 | 4.2084e+0 | 2.0495e+0 | **1.5287e+0** |
| | | (3.22e-1) - | (1.76e-1)+ | (3.20e-1) - | (2.57e-1) - | (2.12e+0) - | (2.01e-1) = | (6.75e-1) - | (5.81e-1) - | (4.21e-1) - | **(1.38e-1)** |
| | 15 | 5.9272e+0 | 4.0840e+0 | 5.4110e+0 | 3.1135e+0 | 1.1798e+1 | 4.3868e+0 | 3.5246e+0 | 6.6735e+0 | 3.4725e+0 | **1.5617e+0** |
| | | (7.57e-1) - | (1.40e+0)+ | (5.71e-1) - | (3.48e-1) - | (2.94e+0) - | (1.43e+0) - | (6.45e-1) - | (2.58e-1) - | (8.29e-1) - | **(7.55e-1)** |
| WFG4 | 3 | 2.4559e-1 | 3.0927e-1 | 3.3570e-1 | 2.3828e-1 | 2.8015e-1 | 2.3478e-1 | 2.1577e-1 | 3.3229e-1 | 2.9084e-1 | 1.9636e-1 |
| | | (6.84e-3) - | (7.07e-3) - | (1.36e-2) - | (4.58e-3) - | (5.97e-3) - | (4.28e-3) - | (2.03e-3) - | (1.91e-2) - | (9.23e-3) - | (3.12e-3) |
| | 5 | 1.2159e+0 | 1.8606e+0 | 2.2318e+0 | 1.3569e+0 | 1.3559e+0 | 1.2351e+0 | 1.2134e+0 | 1.4091e+0 | 1.3352e+0 | **1.0642e+0** |
| | | (1.19e-2) - | (7.69e-2) - | (6.29e-2) - | (3.76e-2) - | (1.30e-2) - | (6.70e-3) - | (1.09e-2) - | (2.60e-2) - | (3.24e-2) - | **(1.46e-2)** |
| | 10 | 4.8809e+0 | 1.0762e+1 | 7.5327e+0 | 5.2605e+0 | 5.8685e+0 | 6.1805e+0 | 5.3421e+0 | 6.1955e+0 | 5.1647e+0 | **4.8128e+0** |
| | | (3.50e-2) - | (7.65e-1) - | (2.07e-1) - | (8.49e-2) - | (1.47e-1) - | (7.12e-2) - | (5.80e-2) - | (2.83e-1) - | (8.04e-2) - | **(9.66e-2)** |
| | 15 | 8.8065e+0 | 2.4012e+1 | 1.4530e+1 | 8.9336e+0 | 1.1409e+1 | 1.3150e+1 | 8.7425e+0 | 1.2015e+1 | 9.1672e+0 | **8.5907e+0** |
| | | (9.00e-2) - | (1.10e+0) - | (2.08e+0) - | (9.70e-2) - | (3.00e-1) - | (2.82e-1) - | (1.95e-1) - | (7.41e-1) - | (6.83e-2) - | **(1.55e-1)** |
| WFG5 | 3 | 2.3929e-1 | 3.1338e-1 | 2.8843e-1 | 2.4583e-1 | 2.5194e-1 | 2.3583e-1 | 2.2557e-1 | 2.7419e-1 | 2.7967e-1 | **2.0908e-1** |
| | | (3.50e-3) - | (9.67e-3) - | (6.25e-3) - | (5.36e-3) - | (3.44e-3) - | (1.46e-3) - | (2.12e-3) - | (2.29e-2) - | (8.97e-3) - | **(2.43e-3)** |
| | 5 | 1.2009e+0 | 1.7904e+0 | 2.0061e+0 | 1.3207e+0 | 1.3363e+0 | 1.2222e+0 | 1.2094e+0 | 1.3573e+0 | 1.4765e+0 | **1.0741e+0** |
| | | (1.28e-2) - | (5.76e-2) - | (5.69e-2) - | (2.10e-2) - | (1.17e-2) - | (9.08e-3) - | (1.16e-2) - | (3.53e-2) - | (1.12e-1) - | **(1.07e-2)** |
| | 10 | **4.7597e+0** | 1.0071e+1 | 7.0964e+0 | 5.4419e+0 | 5.6243e+0 | 6.1003e+0 | 5.3459e+0 | 5.7432e+0 | 5.5064e+0 | 4.8875e+0 |
| | | **(3.38e-2)+** | (8.46e-1) - | (2.05e-1) - | (1.02e-1) - | (1.69e-1) - | (5.85e-2) - | (6.02e-2) - | (1.13e-1) - | (1.13e-1) - | (8.18e-2) |
| | 15 | 8.4761e+0 | 2.2514e+1 | 1.8419e+1 | 9.0057e+0 | 1.3618e+1 | 1.2508e+1 | 8.5726e+0 | 1.3096e+1 | 1.1762e+1 | **8.4706e+0** |
| | | (8.53e-2) = | (1.34e+0) - | (2.07e+0) - | (1.20e-1) - | (3.95e+0) - | (1.64e-1) - | (1.55e-1) - | (1.36e+0) - | (3.81e-1) - | **(1.55e-1)** |
| WFG6 | 3 | 2.5738e-1 | 3.7902e-1 | 3.4907e-1 | 2.5820e-1 | 2.6426e-1 | 2.6278e-1 | 2.3792e-1 | 3.7588e-1 | 3.0172e-1 | **2.3471e-1** |
| | | (2.64e-2) - | (1.89e-2) - | (2.67e-2) - | (6.90e-3) - | (1.87e-2) - | (1.58e-2) - | (1.05e-2) = | (1.88e-2) - | (1.53e-2) - | **(1.20e-2)** |
| | 5 | 1.2911e+0 | 1.9489e+0 | 2.0061e+0 | 1.3509e+0 | 1.5231e+0 | 1.2593e+0 | 1.2475e+0 | 1.4306e+0 | 1.4870e+0 | **1.0990e+0** |
| | | (2.72e-2) - | (8.98e-2) - | (1.94e-1) - | (3.12e-2) - | (1.12e-1) - | (1.62e-2) - | (1.65e-2) - | (4.24e-2) - | (5.91e-2) - | **(1.13e-2)** |
| | 10 | **4.9599e+0** | 1.0032e+1 | 7.4407e+0 | 5.6154e+0 | 7.3553e+0 | 6.2516e+0 | 5.5019e+0 | 8.6133e+0 | 5.3422e+0 | 5.2791e+0 |
| | | **(4.53e-2)+** | (7.64e-1) - | (2.25e-1) - | (9.84e-2) - | (3.42e-1) - | (6.11e-2) - | (5.12e-2) - | (1.94e+0) - | (7.85e-2) - | (8.72e-2) |
| | 15 | 8.7252e+0 | 2.2611e+1 | 1.8745e+1 | 9.1626e+0 | 1.3890e+1 | 1.3051e+1 | 8.8122e+0 | 1.4331e+1 | 9.4249e+0 | **9.2576e+0** |
| | | (4.15e-3) - | (1.31e-2) - | (1.58e-2) - | (7.50e-3) - | (2.35e-2) - | (5.05e-3) - | (1.95e-3) - | (3.04e-2) - | (2.76e-1) = | **(2.83e-3)** |
| WFG7 | 3 | 2.0150e-1 | 2.6248e-1 | 2.7881e-1 | 2.1179e-1 | 2.2668e-1 | 2.2119e-1 | 2.0143e-1 | 2.8771e-1 | 2.8318e-1 | **2.1050e-1** |
| | | (3.15e-3) - | (1.02e-2) - | (1.08e-2) - | (3.23e-3) - | (5.55e-3) - | (2.01e-3) - | (1.95e-3) - | (2.06e-2) - | (9.45e-3) - | **(2.83e-3)** |
| | 5 | 1.2363e+0 | 1.8716e+0 | 2.2011e+0 | 1.3662e+0 | 1.3925e+0 | 1.2575e+0 | 1.2333e+0 | 1.4821e+0 | 1.3900e+0 | **1.0892e+0** |
| | | (1.39e-2) - | (8.23e-2) - | (1.00e-1) - | (3.44e-2) - | (1.44e-2) - | (1.19e-2) - | (1.34e-2) - | (4.28e-2) - | (3.14e-2) - | **(1.11e-2)** |
| | 10 | **4.8709e+0** | 1.0022e+1 | 7.4223e+0 | 5.5017e+0 | 5.8906e+0 | 6.1628e+0 | 5.3753e+0 | 5.8382e+0 | 5.3197e+0 | 5.0131e+0 |
| | | **(3.18e-2)+** | (7.04e-1) - | (2.57e-1) - | (8.87e-2) - | (1.57e-1) - | (7.76e-2) - | (8.69e-2) - | (1.72e-1) - | (9.54e-2) - | (1.03e-1) |
| | 15 | 8.7052e+0 | 2.2885e+1 | 2.0396e+1 | 8.9953e+0 | 1.2668e+1 | 1.3099e+1 | 8.9678e+0 | 1.1496e+1 | 1.1129e+1 | **8.5628e+0** |
| | | (6.89e-2) - | (1.61e+0) - | (1.68e+0) - | (1.69e-1) - | (2.27e+0) - | (2.41e-1) - | (3.36e-1) - | (6.45e-1) - | (2.35e-1) - | **(1.20e-1)** |
| +/ − / = | | 5/22/1 | 1/27/0 | 0/28/0 | 2/24/2 | 1/27/0 | 1/24/3 | 3/24/1 | 0/27/1 | 2/25/1 | |

**Table 3.** IGD values on MaF test problems.

| Problem | M | IGD | | | | | | | | | |
|---|---|---|---|---|---|---|---|---|---|---|---|
| | | CMOEA-CD | IMC-MOEAD | LERD | NRVMOEA | FDV | HEA | LMPFE | DGEA | NSGAII-ARSBX | DES-NSGA-II |
| MaF1 | 3 | 4.9674e-2 | 1.0147e-1 | 8.0318e-2 | 4.3790e-2 | 8.4195e-2 | 7.1137e-2 | 4.4484e-2 | 1.1327e-1 | 5.9424e-2 | **4.3721e-2** |
| | | (1.85e-3) - | (1.12e-2) - | (2.32e-3) - | (4.31e-4) = | (9.88e-4) - | (4.16e-4) - | (6.23e-4) - | (8.68e-3) - | (2.72e-3) - | **(1.02e-3)** |
| | 5 | 1.8375e-1 | 2.0548e-1 | 2.4655e-1 | 1.3853e-1 | 3.5323e-1 | 2.2642e-1 | **1.3629e-1** | 4.3198e-1 | 1.8621e-1 | 1.5746e-1 |
| | | (9.00e-3) - | (1.36e-2) - | (9.06e-3) - | (3.17e-3)+ | (2.81e-2) - | (6.51e-3) - | **(3.13e-3)+** | (4.40e-2) - | (6.51e-3) - | (2.48e-3) |
| | 10 | 4.2339e-1 | 3.8010e-1 | 4.1652e-1 | **2.6509e-1** | 5.9817e-1 | 3.5691e-1 | 2.7303e-1 | 6.7739e-1 | 3.4025e-1 | 3.0942e-1 |
| | | (2.15e-2) - | (3.62e-2) - | (3.22e-2) - | **(1.09e-2)+** | (6.29e-2) - | (2.20e-2) - | (2.64e-2)+ | (1.03e-1) - | (1.28e-2) - | (4.69e-3) |
| | 15 | 6.0913e-1 | 4.7328e-1 | 5.2350e-1 | 3.7151e-1 | 7.5374e-1 | 4.6918e-1 | 3.5789e-1 | 8.7013e-1 | 3.9695e-1 | **3.4061e-1** |
| | | (6.78e-2) - | (3.89e-2) - | (4.44e-2) - | (2.23e-2) - | (9.68e-2) - | (4.38e-2) - | (2.74e-2) - | (1.44e-1) - | (1.59e-2) - | **(3.00e-3)** |
| MaF2 | 3 | 4.4869e-2 | 4.4808e-2 | 4.6732e-2 | 3.1396e-2 | 3.9277e-2 | 3.6751e-2 | 3.0115e-2 | 4.3261e-2 | 5.1983e-2 | **2.8890e-2** |
| | | (1.31e-3) - | (7.89e-4) - | (1.26e-3) - | (3.91e-4) - | (5.97e-4) - | (1.67e-4) - | (3.98e-4) - | (2.28e-3) - | (2.61e-3) - | **(7.83e-4)** |
| | 5 | 1.2685e-1 | 1.5242e-1 | 2.0356e-1 | 1.1421e-1 | 1.8101e-1 | 1.4128e-1 | **1.1130e-1** | 1.4531e-1 | 1.4932e-1 | 1.1678e-1 |
| | | (2.85e-3) - | (3.10e-3) - | (1.07e-2) - | (2.34e-3)+ | (5.89e-2) - | (1.56e-3) - | **(2.21e-3)+** | (4.38e-3) - | (3.98e-3) - | (3.05e-3) |
| | 10 | 1.8809e-1 | 5.0142e-1 | 3.4499e-1 | **1.7927e-1** | 8.5658e-1 | 2.1707e-1 | 1.9926e-1 | 4.6501e-1 | 1.8964e-1 | 2.0446e-1 |
| | | (2.36e-3)+ | (7.10e-2) - | (2.39e-2) - | **(5.10e-3)+** | (1.22e-2) - | (3.50e-3) - | (6.02e-2)+ | (1.13e-1) - | (2.96e-3)+ | (7.75e-3) |
| | 15 | 2.0361e-1 | 6.4436e-1 | 6.4737e-1 | 2.1535e-1 | 8.9291e-1 | 2.6287e-1 | 2.8568e-1 | 6.4111e-1 | **1.8964e-1** | 3.0990e-1 |
| | | (3.37e-3)+ | (7.18e-2) - | (5.40e-2) - | (1.01e-2)+ | (5.05e-3) - | (1.75e-2) - | (5.11e-2) = | (1.33e-1) - | **(2.49e-3)+** | (3.85e-2) |
| MaF3 | 3 | **3.4827e-1** | 9.5238e+3 | 1.0903e+4 | 1.1864e+2 | 4.2502e-2 | 1.4110e+3 | 1.2463e+2 | 2.1312e+4 | 8.4003e+3 | 8.5747e-1 |
| | | **(7.98e-1)+** | (6.07e+3) - | (1.45e+4) - | (1.22e+2) - | (1.42e-3)+ | (4.11e+3) - | (1.61e+2) - | (1.63e+4) - | (4.97e+3) - | (1.69e+0) |
| | 5 | 1.5857e+1 | 1.5107e+4 | 1.8921e+6 | 5.7742e+3 | **1.6996e-1** | 3.2573e+3 | 2.5796e+3 | 2.0674e+4 | 5.0853e+4 | 2.8417e-1 |
| | | (2.05e+1) - | (1.45e+4) - | (1.03e+7) - | (5.26e+3) - | **(3.41e-1)+** | (6.75e+3) - | (2.32e+3) - | (1.74e+4) - | (2.92e+4) - | (4.58e-1) |
| | 10 | 3.1383e+2 | 5.4742e+5 | 4.5967e+6 | 2.0346e+9 | **3.0745e-1** | 1.4950e+3 | 1.9238e+3 | 2.4562e+4 | 2.2993e+8 | 3.5712e+0 |
| | | (6.53e+2) - | (1.28e+6) - | (2.51e+7) - | (2.64e+9) - | **(4.03e-1) =** | (5.44e+3) - | (6.79e+3) - | (1.66e+4) - | (1.21e+9) - | (9.28e+0) |
| | 15 | 3.7727e+3 | 4.5538e+6 | 1.0393e+8 | 2.0065e+9 | **2.7026e-1** | 2.4969e+3 | 1.8842e+5 | 1.3833e+4 | 4.4376e+6 | 3.4361e-1 |
| | | (8.97e+3) - | (1.41e+7) - | (2.69e+8) - | (2.87e+9) - | **(7.90e-2) =** | (1.26e+4) - | (8.60e+4) - | (1.56e+4) - | (6.55e+6) - | (2.58e-1) |
| MaF4 | 3 | 1.2329e+0 | 1.5851e+2 | 6.2677e+1 | 2.3053e+1 | **4.8117e-1** | 1.7676e+1 | 2.0065e+1 | 3.7800e+2 | 3.0455e+2 | 8.4949e-1 |
| | | (1.84e+0) = | (4.21e+1) - | (6.98e+1) - | (1.60e+1) - | **(3.50e-2)+** | (9.69e+0) - | (9.20e+0) - | (1.85e+2) - | (7.90e+1) - | (1.09e+0) |
| | 5 | 1.7964e+1 | 6.4314e+2 | 7.1776e+2 | 1.8519e+2 | **1.8692e+0** | 9.1341e+1 | 4.3123e+2 | 1.0672e+3 | 1.6231e+3 | 3.1540e+0 |
| | | (2.22e+1) - | (2.10e+2) - | (5.46e+2) - | (8.87e+1) - | **(1.91e-1) -** | (7.81e+1) - | (1.55e+3) - | (5.95e+2) - | (3.67e+2) - | (2.98e-1) |
| | 10 | 1.1817e+3 | 2.4165e+4 | 2.4994e+4 | 4.8913e+2 | **4.0789e+1** | 3.5726e+3 | 1.9844e+3 | 4.3249e+4 | 6.9150e+4 | 1.2195e+2 |
| | | (9.92e+2) - | (9.30e+3) - | (1.79e+4) - | (2.22e+3) - | **(2.67e+0)+** | (3.25e+3) - | (6.79e+3) - | (2.64e+4) - | (1.91e+4) - | (2.08e+1) |
| | 15 | 1.0843e+4 | 8.3571e+5 | 1.1916e+6 | 2.2209e+5 | 1.2235e+4 | 1.8180e+5 | 2.0465e+5 | 1.5671e+6 | 1.4688e+5 | **9.9833e+2** |
| | | (1.69e+4) - | (4.16e+5) - | (7.02e+5) - | (1.34e+5) - | (8.96e+2) - | (1.28e+5) - | (1.56e+5) - | (1.17e+6) - | (9.40e+4) - | **(7.31e+2)** |
| MaF5 | 3 | **2.5793e-1** | 6.4963e-1 | 1.2520e+0 | 9.8183e-1 | 6.9577e-1 | 1.3695e+0 | 9.3589e-1 | 8.4226e-1 | 3.0070e-1 | 6.6385e-1 |
| | | **(4.30e-3)+** | (2.80e-1)+ | (1.92e+0) - | (1.03e+0) - | (3.63e-1) - | (1.40e+0) - | (1.06e+0) - | (4.71e-1) - | (9.31e-3)+ | (1.03e+0) |
| | 5 | 2.3428e+0 | 7.2978e+0 | 4.2552e+0 | 2.4711e+0 | 5.0290e+0 | 3.4541e+0 | 2.7400e+0 | 5.3599e+0 | 2.6978e+0 | **2.1684e+0** |
| | | (4.15e-2) - | (9.03e-1) - | (5.54e-1) - | (8.17e-2) - | (9.19e-1) - | (1.54e+0) - | (6.55e-1) - | (9.73e-1) - | (9.45e-2) - | **(3.27e-1)** |
| | 10 | 8.1783e+1 | 4.6783e+2 | 1.9206e+2 | 8.3012e+1 | 2.1586e+2 | 1.2474e+2 | 7.2741e+4 | 2.6104e+2 | 1.2398e+2 | **6.5073e+1** |
| | | (2.10e+1) - | (2.44e+2) - | (2.70e+1) - | (7.61e+0) - | (4.42e+1) - | (2.14e+1) - | (3.73e+5) - | (2.36e+1) - | (1.32e+1) - | **(4.26e+0)** |
| | 15 | 2.1337e+3 | 1.7508e+4 | 6.2350e+3 | 2.7786e+3 | 6.2500e+3 | 3.6009e+3 | 4.0958e+3 | 7.0533e+3 | 2.8425e+3 | **1.5567e+3** |
| | | (3.24e+2) - | (8.13e+3) - | (5.22e+2) - | (3.14e+2) - | (9.16e+2) - | (3.86e+2) - | (1.15e+3) - | (2.96e+2) - | (2.85e+2) - | **(1.46e+2)** |
| MaF6 | 3 | **4.1622e-3** | 2.6069e-1 | 2.4123e-2 | 7.3251e-3 | 3.3144e-2 | 4.6584e-2 | 9.6212e-3 | 7.8631e-2 | 5.3654e-3 | 5.7881e-3 |
| | | **(3.59e-5)+** | (6.74e-2) - | (7.73e-4) - | (2.57e-3) - | (1.11e-3) - | (9.63e-3) - | (1.64e-2) - | (2.39e-2) - | (1.80e-4)+ | (6.02e-4) |
| | 5 | **4.3697e-3** | 3.0955e-1 | 1.4963e-1 | 6.5580e-3 | 8.8163e-2 | 6.9190e-2 | 1.1866e-2 | 1.1822e-1 | 6.0909e-3 | 9.0988e-3 |
| | | **(7.81e-5)+** | (9.31e-2) - | (3.33e-2) - | (1.97e-3)+ | (4.95e-4) - | (3.89e-3) - | (1.53e-2) - | (3.13e-2) - | (3.55e-4)+ | (1.71e-3) |
| | 10 | 3.4006e-1 | 1.0379e+0 | 2.9424e-1 | 7.2005e-1 | 5.6740e-1 | 7.4757e-1 | 7.9449e-1 | **1.3504e-1** | 5.3115e+0 | 2.3682e-1 |
| | | (1.19e-1) - | (7.03e-1) - | (6.01e-3) = | (4.60e-1) - | (2.42e-1) - | (8.22e-1) = | (1.29e+0) = | **(5.90e-2)+** | (2.86e+0) - | (1.23e-1) |
| | 15 | 3.7039e-1 | 1.0690e+0 | 3.1262e-1 | 8.5908e+0 | 6.8573e-1 | 5.3924e-1 | 4.9119e+0 | 5.2914e-1 | 5.7512e-1 | **2.9873e-1** |
| | | (1.07e-1) - | (9.05e-1) - | (2.61e-2) - | (4.79e+0) - | (1.03e-1) - | (1.30e+0) = | (2.43e+0) - | (3.05e-1) - | (2.12e-1) - | **(8.26e-2)** |
| MaF7 | 3 | **6.0953e-2** | 2.1521e-1 | 8.0061e-1 | 1.2282e-1 | 6.6265e-1 | 1.5435e-1 | 2.0023e-1 | 2.4646e+0 | 8.3087e-2 | 7.7566e-2 |
| | | **(1.00e-3)+** | (4.65e-2) - | (7.93e-2) - | (1.20e-1) - | (2.17e-1) - | (1.83e-1) - | (2.10e-1) - | (1.50e+0) - | (3.06e-3) - | (7.44e-2) |
| | 5 | 3.7550e-1 | 9.3203e-1 | 1.3434e+0 | 3.1760e-1 | 1.1355e+0 | 1.3811e+0 | 1.2420e+0 | 1.4741e+0 | 1.2358e+0 | **3.0838e-1** |
| | | (1.06e-2) - | (1.95e-1) - | (4.13e-1) - | (9.15e-2) - | (3.48e-1) - | (8.74e-1) - | (3.97e-1) - | (7.43e-1) - | (2.77e-1) - | **(1.33e-2)** |
| | 10 | 1.7023e+0 | 2.0607e+1 | 5.7295e+0 | **8.8240e-1** | 2.0111e+0 | 5.8769e+0 | 2.5424e+0 | 2.0618e+0 | 3.7128e+0 | 1.0922e+0 |
| | | (1.75e-1) - | (4.18e+0) - | (1.04e+0) - | **(1.53e-2)+** | (5.31e-1) - | (9.22e-1) - | (2.92e+0) - | (4.32e-1) - | (2.10e+0) - | (1.13e-1) |
| | 15 | 4.8531e+0 | 2.5630e+1 | 1.5013e+1 | 1.4524e+1 | 3.5120e+0 | 1.2067e+1 | 3.3695e+1 | **3.7415e+0** | 3.6407e+0 | 5.6553e+0 |
| | | (1.07e+0)+ | (5.20e+0) - | (4.84e+0) - | (2.00e+0) - | (9.78e-1)+ | (4.87e-1) - | (5.12e+0) - | **(8.99e-1)+** | (1.69e+0)+ | (3.19e-1) |
| +/ − / = | | 9/18/1 | 0/28/0 | 0/26/2 | 7/20/1 | 4/22/2 | 1/25/2 | 4/22/2 | 2/26/0 | 6/22/0 | |

**Table 4.** IGD+ values on DTLZ test problems.

| Problem | M | IGD+ | | | | | | | | | |
|---|---|---|---|---|---|---|---|---|---|---|---|
| | | CMOEA-CD | IMC-MOEAD | LERD | NRVMOEA | FDV | HEA | LMPFE | DGEA | NSGAII-ARSBX | DES-NSGA-II |
| DTLZ1 | 3 | **1.4605e-2** | 3.9246e+0 | 7.5003e-1 | 8.9108e-2 | 1.5697e-2 | 1.0335e-1 | 1.6482e-1 | 1.2838e+1 | 1.8635e+0 | 1.7829e-2 |
| | | **(5.80e-4)+** | (1.51e+0) - | (1.41e+0) - | (1.08e-1) - | (1.23e-3)+ | (1.58e-1) - | (1.78e-1) - | (7.63e+0) - | (1.93e+0) - | (1.44e-3) |
| | 5 | 3.1565e-1 | 3.8847e+0 | 1.8194e+0 | 6.5932e-1 | 5.3251e-2 | 2.5770e-1 | 7.7405e-1 | 9.6530e+0 | 1.6137e+1 | **4.6635e-2** |
| | | (1.03e+0) - | (1.74e+0) - | (2.15e+0) - | (4.38e-1) - | (7.54e-3) - | (2.71e-1) - | (4.71e-1) - | (8.14e+0) - | (5.86e+0) - | **(1.56e-3)** |
| | 10 | 2.3253e-1 | 4.3369e+0 | 2.8481e+0 | 6.3331e+0 | 1.7938e-1 | 6.0694e-1 | 1.2161e+1 | 7.8634e+0 | 2.6508e+1 | **8.5606e-2** |
| | | (1.16e-1) - | (2.76e+0) - | (2.40e+0) - | (2.63e+0) - | (4.81e-1) = | (7.20e-1) - | (7.00e+0) - | (3.98e+0) - | (9.43e+0) - | **(5.47e-3)** |
| | 15 | 2.3043e-1 | 8.6113e+0 | 7.4366e+0 | 6.6080e+0 | 1.3199e-1 | 5.6783e-1 | 7.2026e+0 | 6.2067e+0 | 3.8076e+0 | **1.0957e-1** |
| | | (6.77e-2) - | (3.59e+0) - | (7.32e+0) - | (3.37e+0) - | (5.91e-2) = | (6.75e-1) - | (3.03e+0) - | (3.91e+0) - | (2.28e+0) - | **(9.75e-3)** |
| DTLZ2 | 3 | 2.5827e-2 | 7.6850e-2 | 3.4409e-2 | 2.4569e-2 | 2.9261e-2 | 2.3564e-2 | 2.5390e-2 | 9.0653e-2 | 3.9672e-2 | **2.0876e-2** |
| | | (7.36e-4) - | (5.77e-3) - | (1.85e-3) - | (4.51e-4) - | (2.07e-3) - | (2.45e-4) - | (4.53e-4) - | (1.50e-2) - | (2.36e-3) - | **(4.26e-4)** |
| | 5 | 1.1355e-1 | 2.8762e-1 | 2.5283e-1 | 8.4279e-2 | 1.8660e-1 | 8.8443e-2 | 9.5023e-2 | 2.9166e-1 | 4.8003e-1 | **7.5488e-2** |
| | | (6.19e-3) - | (2.53e-2) - | (4.00e-2) - | (1.50e-3) - | (1.40e-2) - | (1.02e-3) - | (5.67e-3) - | (2.99e-2) - | (1.28e-1) - | **(1.36e-3)** |
| | 10 | 3.3877e-1 | 6.4136e-1 | 6.9448e-1 | 2.0340e-1 | 4.5479e-1 | 2.0111e-1 | 2.4837e-1 | 5.8091e-1 | 1.2485e+0 | **1.7587e-1** |
| | | (3.52e-2) - | (4.74e-2) - | (5.79e-2) - | (5.17e-3) - | (5.10e-2) - | (3.03e-3) - | (3.97e-2) - | (4.35e-2) - | (1.41e-1) - | **(2.11e-3)** |
| | 15 | 4.6425e-1 | 7.7503e-1 | 8.2204e-1 | 2.9906e-1 | 7.1225e-1 | 3.5092e-1 | 2.9235e-1 | 7.9603e-1 | 2.3732e+0 | **2.6494e-1** |
| | | (6.37e-2) - | (2.40e-2) - | (7.90e-2) - | (1.49e-2) - | (7.17e-2) - | (1.69e-2) - | (6.16e-2) = | (6.48e-2) - | (3.14e-1) - | **(3.86e-3)** |
| DTLZ3 | 3 | 2.4190e-1 | 6.5102e+1 | 3.7111e+1 | 7.5098e+0 | **2.5538e-2** | 6.8561e+0 | 7.4166e+0 | 8.6531e+1 | 8.0822e+1 | 3.0100e-1 |
| | | (4.79e-1)+ | (1.27e+1) - | (3.58e+1) - | (4.79e+0) - | **(2.38e-3)+** | (5.14e+0) - | (4.99e+0) - | (4.65e+1) - | (6.47e+1) - | (4.28e-1) |
| | 5 | 7.6905e-1 | 7.6235e+1 | 2.9379e+1 | 2.9623e+1 | 3.4438e-1 | 4.7059e+0 | 3.2850e+1 | 7.6556e+1 | 1.5298e+2 | **2.1962e-1** |
| | | (8.45e-1) - | (1.99e+1) - | (2.85e+1) - | (1.03e+1) - | (2.41e-1) - | (2.96e+0) - | (1.15e+1) - | (4.00e+1) - | (2.63e+1) - | **(3.02e-1)** |
| | 10 | 2.6963e+0 | 7.7264e+1 | 6.3688e+1 | 1.0586e+2 | 6.9716e-1 | 6.7999e+0 | 2.4682e+2 | 8.6859e+1 | 6.7654e+2 | **2.1730e-1** |
| | | (2.00e+0) - | (1.48e+1) - | (4.38e+1) - | (2.17e+1) - | (3.59e-1) - | (4.37e+0) - | (1.20e+2) - | (4.72e+1) - | (2.65e+2) - | **(1.31e-2)** |
| | 15 | 3.4134e+0 | 6.6708e+1 | 8.6094e+1 | 1.4283e+2 | 7.6213e-1 | 8.8297e+0 | 7.2403e+1 | 5.8402e+1 | 7.6697e+2 | **2.9975e-1** |
| | | (3.42e+0) - | (1.80e+1) - | (6.08e+1) - | (2.99e+1) - | (3.34e-2) - | (7.53e+0) - | (5.17e+1) - | (4.40e+1) - | (4.31e+2) - | **(5.81e-2)** |
| DTLZ4 | 3 | **2.5962e-2** | 1.2987e-1 | 3.2174e-1 | 1.0842e-1 | 7.2567e-2 | 1.1545e-1 | 9.2090e-2 | 1.3391e-1 | 3.7653e-2 | 7.5675e-2 |
| | | **(9.49e-4)+** | (7.04e-2) - | (5.08e-1) - | (1.23e-1) - | (6.65e-2)+ | (1.58e-1) - | (1.39e-1) - | (7.07e-2) - | (1.51e-3)+ | (9.23e-2) |
| | 5 | 1.0580e-1 | 3.0889e-1 | 1.4547e-1 | 9.3217e-2 | 1.4952e-1 | 2.3900e-1 | 1.2154e-1 | 2.7292e-1 | 2.0779e-1 | **7.5196e-2** |
| | | (4.81e-3) - | (4.91e-2) - | (2.63e-2) - | (3.85e-2) - | (2.04e-2) - | (1.17e-1) - | (2.65e-2) - | (4.94e-2) - | (1.96e-2) - | **(1.16e-3)** |
| | 10 | 3.1462e-1 | 7.7673e-1 | 3.2222e-1 | 1.9113e-1 | 2.6460e-1 | 2.9607e-1 | 5.5509e-1 | 4.6053e-1 | 1.3059e+0 | **1.6903e-1** |
| | | (2.44e-2) - | (3.29e-2) - | (3.19e-2) - | (4.66e-3) - | (1.87e-2) - | (5.17e-2) - | (1.03e-1) - | (4.19e-2) - | (1.92e-1) - | **(1.79e-3)** |
| | 15 | 4.2213e-1 | 8.4541e-1 | 6.6237e-1 | 2.6261e-1 | 3.6691e-1 | 4.9364e-1 | 3.5425e-1 | 5.3448e-1 | 2.2190e+0 | **2.5731e-1** |
| | | (3.26e-2) - | (4.16e-2) - | (7.04e-2) - | (7.41e-3) - | (2.36e-2) - | (6.16e-2) - | (1.43e-1) - | (4.35e-2) - | (1.64e-1) - | **(3.94e-3)** |
| DTLZ5 | 3 | 4.2608e-3 | 2.0611e-2 | 1.0180e-2 | 2.6632e-3 | 1.4980e-2 | 1.4404e-2 | **2.6407e-3** | 3.3949e-2 | 3.6180e-3 | 3.2250e-3 |
| | | (5.24e-4) - | (4.52e-3) - | (3.30e-4) - | (2.56e-4)+ | (1.01e-3) - | (8.73e-4) - | **(2.09e-4)+** | (1.19e-2) - | (3.43e-4) - | (2.47e-4) |
| | 5 | 1.7154e-1 | 5.0719e-2 | 1.1483e-1 | 6.4520e-2 | 4.7517e-2 | 5.7328e-2 | 1.1538e-1 | 1.0639e-1 | 1.3469e-1 | **3.1754e-2** |
| | | (4.33e-2) - | (9.02e-3) - | (4.05e-2) - | (1.82e-2) - | (1.40e-2) - | (1.82e-2) - | (4.20e-2) - | (4.62e-2) - | (5.21e-2) - | **(1.07e-2)** |
| | 10 | 3.2573e-1 | 2.5050e-1 | 2.2489e-1 | 1.5159e-1 | 3.0537e-1 | 1.5650e-1 | 2.4421e-1 | **7.1028e-2** | 4.5508e-1 | 9.1396e-2 |
| | | (9.35e-2) - | (9.04e-2) - | (3.63e-2) - | (3.30e-2) - | (1.33e-1) - | (5.39e-2) - | (1.06e-1) - | **(2.63e-2) =** | (1.25e-1) - | (3.99e-2) |
| | 15 | 2.6745e-1 | 1.9174e-1 | 2.5553e-1 | 1.0279e-1 | 3.7608e-1 | 1.6248e-1 | 3.4245e-1 | 2.3848e-1 | 3.2107e-1 | **9.5835e-2** |
| | | (1.36e-1) - | (7.09e-2) - | (5.81e-2) - | (5.23e-2) = | (3.12e-3) - | (6.96e-2) - | (1.33e-1) - | (1.31e-1) - | (9.08e-2) - | **(4.68e-2)** |
| DTLZ6 | 3 | **1.7803e-3** | 4.6424e+0 | 9.0380e-3 | 2.1872e-3 | 1.5530e+0 | 1.7520e-2 | 2.0070e-3 | 1.1672e+0 | 2.3657e-3 | 2.7194e-3 |
| | | **(2.17e-5)+** | (1.76e-1) - | (1.48e-4) - | (5.07e-4)+ | (9.63e-1) - | (1.08e-3) - | (3.82e-5)+ | (1.13e+0) - | (1.13e-4)+ | (2.05e-4) |
| | 5 | 8.5332e-2 | 4.3434e+0 | 7.7607e-2 | 2.4122e-1 | 2.7731e+0 | 3.3815e-1 | 1.9407e+0 | 2.0458e+0 | 3.2041e+0 | **5.7314e-2** |
| | | (5.68e-2) - | (2.12e-1) - | (6.36e-2) - | (2.93e-1) - | (1.07e+0) - | (2.71e-1) - | (7.55e-1) - | (1.10e+0) - | (1.02e+0) - | **(1.92e-2)** |
| | 10 | 3.0626e-1 | 4.1686e+0 | 2.6346e-1 | 1.1542e+0 | 3.3224e+0 | 1.5763e+0 | 4.6341e+0 | 1.6450e+0 | 5.5005e+0 | **1.1311e-1** |
| | | (2.23e-1) - | (2.86e-1) - | (1.65e-1) = | (5.37e-1) - | (1.09e+0) - | (1.17e+0) - | (9.17e-1) - | (9.66e-1) - | (1.08e+0) - | **(6.29e-2)** |
| | 15 | 3.7679e-1 | 6.9442e+0 | 2.9555e-1 | 2.1149e-1 | 1.7022e+0 | 7.1243e-1 | 1.0542e+0 | 8.0998e-1 | 3.1657e+0 | **1.2114e-1** |
| | | (5.65e-17) - | (5.20e-1) - | (4.43e-2) - | (1.05e-1) - | (1.21e+0) - | (4.63e-1) - | (1.48e+0) - | (5.83e-1) - | (1.25e+0) - | **(6.64e-2)** |
| DTLZ7 | 3 | **3.0817e-2** | 1.7341e-1 | 6.2413e-1 | 5.8138e-2 | 5.7331e-1 | 2.0454e-1 | 1.3920e-1 | 1.9155e+0 | 5.7175e-2 | 4.4696e-2 |
| | | **(1.11e-3)+** | (4.77e-2) - | (1.45e-1) - | (6.04e-2) - | (1.84e-1) - | (3.12e-1) - | (1.66e-1) - | (1.03e+0) - | (3.25e-3) - | (4.89e-2) |
| | 5 | 2.1196e-1 | 8.0232e-1 | 1.2173e+0 | 2.0388e-1 | 8.8419e-1 | 1.1495e+0 | 1.1038e+0 | 1.1794e+0 | 1.1827e+0 | **1.4848e-1** |
| | | (1.80e-2) - | (1.68e-1) - | (4.16e-1) - | (5.74e-2) - | (2.57e-1) - | (9.04e-1) - | (4.37e-1) - | (4.65e-1) - | (1.91e-1) - | **(7.55e-3)** |
| | 10 | 1.5117e+0 | 2.1114e+1 | 6.2791e+1 | 1.5496e+0 | 1.4147e+0 | 5.3119e+0 | 1.5009e+1 | 1.6376e+0 | 3.0313e+0 | **8.4191e-1** |
| | | (1.49e-1) - | (4.09e+0) - | (1.27e+0) - | (4.09e-1) - | (2.74e-1) - | (1.29e+0) - | (3.95e+0) - | (5.38e-1) - | (1.76e+0) - | **(1.29e-1)** |
| | 15 | 4.5092e+0 | 2.5857e+1 | 1.5107e+1 | **1.0329e+0** | 2.6203e+0 | 1.1851e+1 | 4.7295e+0 | 2.6280e+0 | 2.6416e+0 | 4.4975e+0 |
| | | (9.71e-1) = | (5.42e+0) - | (5.02e+0) - | **(2.98e-2)+** | (7.08e-1)+ | (2.99e-4) - | (8.24e+0) - | (1.14e+0)+ | (7.43e-1)+ | (1.16e+0) |
| +/ − / = | | 5/22/1 | 0/28/0 | 0/27/1 | 3/24/1 | 4/22/2 | 0/28/0 | 2/25/1 | 1/26/1 | 3/25/0 | |

**Table 5.** IGD+ values on WFG test problems.

| Problem | M | IGD+ | | | | | | | | | |
|---|---|---|---|---|---|---|---|---|---|---|---|
| | | CMOEA-CD | IMC-MOEAD | LERD | NRVMOEA | FDV | HEA | LMPFE | DGEA | NSGAII-ARSBX | DES-NSGA-II |
| WFG1 | 3 | 3.1816e-1 | 1.3824e+0 | 1.2574e+0 | 8.2328e-2 | 1.1207e+0 | 2.9043e-1 | 8.1366e-2 | 1.5608e+0 | **8.1401e-1** | 1.0562e-1 |
| | | (8.31e-2) - | (8.23e-2) - | (1.78e-1) - | (2.48e-2)+ | (2.98e-1) - | (9.37e-2) - | (2.51e-2)+ | (7.01e-2) - | **(9.60e-2) -** | (3.31e-2) |
| | 5 | 6.4352e-1 | 1.9891e+0 | 1.8593e+0 | 1.1679e+0 | 1.4400e+0 | 6.4613e-1 | 1.0313e+0 | 2.0100e+0 | 8.5013e-1 | **2.0358e-1** |
| | | (1.01e-1) - | (1.40e-1) - | (2.17e-1) - | (1.28e-1) - | (2.38e-1) - | (2.03e-1) - | (1.54e-1) - | (1.04e-1) - | (1.16e-1) - | **(3.39e-2)** |
| | 10 | 8.1282e-1 | 2.5929e+0 | 2.6474e+0 | 4.0533e-1 | 1.8011e+0 | 7.6437e-1 | 4.3934e-1 | 2.8274e+0 | 1.2375e+0 | **3.3571e-1** |
| | | (1.89e-1) - | (2.67e-1) - | (2.01e-1) - | (4.56e-2) - | (2.65e-1) - | (2.31e-1) - | (1.40e-1) - | (1.44e-1) - | (1.37e-1) - | **(4.57e-2)** |
| | 15 | 1.0171e+0 | 3.3283e+0 | 3.4740e+0 | 2.5452e+0 | 2.2203e+0 | 1.9194e+0 | 1.8918e+0 | 3.5033e+0 | 2.9550e+0 | **2.8469e-1** |
| | | (2.38e-1) - | (2.38e-1) - | (3.01e-1) - | (2.49e-1) - | (3.92e-1) - | (6.51e-1) - | (2.94e-1) - | (2.35e-1) - | (2.83e-1) - | **(1.73e-2)** |
| WFG2 | 3 | 7.2897e-2 | 1.4773e-1 | 1.1428e-1 | 4.2323e-2 | 1.1952e-1 | 6.6477e-2 | 6.9720e-2 | 3.1004e-1 | 1.1189e-1 | **5.3294e-2** |
| | | (3.99e-3) - | (8.84e-3) - | (2.37e-2) - | (1.85e-3)+ | (1.36e-2) - | (6.15e-3) - | (1.17e-2) - | (6.89e-2) - | (1.49e-2) - | **(5.67e-3)** |
| | 5 | 3.3938e-1 | 6.4751e-1 | 4.9236e-1 | 1.8282e-1 | 2.3508e-1 | 2.3241e-1 | 3.5022e-1 | 5.0654e-1 | 6.1915e-1 | **1.7160e-1** |
| | | (3.34e-2) - | (1.56e-1) - | (1.07e-1) - | (1.23e-2) - | (2.04e-2) - | (1.99e-2) - | (3.56e-2) - | (8.84e-2) - | (9.93e-2) - | **(4.66e-3)** |
| | 10 | 1.1136e+0 | 3.5181e+0 | 1.7486e+0 | 3.4964e-1 | 3.9230e-1 | 6.2373e-1 | 8.9913e-1 | 1.1222e+0 | 1.0524e+0 | **5.5032e-1** |
| | | (1.77e-1) - | (1.12e+0) - | (7.46e-1) - | (5.05e-2) = | (5.87e-2) = | (6.99e-1) = | (2.16e-1) - | (2.52e-1) - | (2.09e-1) - | **(3.38e-1)** |
| | 15 | 1.4131e+0 | 8.1903e+0 | 4.1651e+0 | 8.5238e-1 | 6.2805e-1 | 2.4040e+0 | **6.0976e-1** | 2.4204e+0 | 1.4862e+0 | 2.0803e-1 |
| | | (3.05e-1)+ | (2.63e+0) - | (1.03e+0) - | (1.81e-1)+ | (2.37e-1)+ | (1.60e+0) = | **(1.77e-1)+** | (4.82e-1) - | (4.82e-1)+ | (6.03e-1) |
| WFG3 | 3 | 1.4187e-1 | 1.6001e-1 | 1.4586e-1 | 6.0989e-2 | 2.1789e-1 | **5.5642e-2** | 8.8357e-2 | 3.7329e-1 | 1.0627e-1 | 8.4003e-2 |
| | | (1.63e-2) - | (1.05e-2) - | (3.86e-2) - | (7.60e-3)+ | (3.92e-2) - | **(9.68e-3)+** | (1.01e-2) = | (4.72e-2) - | (1.33e-2) - | (7.93e-3) |
| | 5 | 7.2317e-1 | **3.0834e-1** | 6.3676e-1 | 5.0151e-1 | 9.8690e-1 | 3.5188e-1 | 6.4235e-1 | 1.0385e+0 | 3.7845e-1 | 3.7367e-1 |
| | | (1.29e-1) - | **(5.05e-2)+** | (1.17e-1) - | (3.89e-2) - | (1.97e-1) - | (5.01e-2) = | (8.96e-2) - | (1.71e-1) - | (7.15e-2) - | (6.23e-2) |
| | 10 | 2.3422e+0 | 9.6779e-1 | 2.0033e+0 | 1.0030e+0 | 2.9819e+0 | **9.4373e-1** | 2.1330e+0 | 2.7984e+0 | 1.4178e+0 | 1.0919e-1 |
| | | (3.32e-1) - | (1.30e-1)+ | (3.14e-1) - | (1.48e-1) - | (3.33e-1) - | **(1.18e-1)+** | (4.67e-1) - | (1.10e-1) - | (2.88e-1) - | (1.17e-1) |
| | 15 | 3.4871e+0 | 2.9522e+0 | 4.3080e+0 | 2.1986e+0 | 4.1807e+0 | 2.8242e+0 | 2.3101e+0 | 4.0937e+0 | 2.2269e+0 | **9.7389e-1** |
| | | (3.29e-1) - | (1.02e+0) - | (5.43e-1) - | (1.97e-1) - | (2.21e-1) - | (8.89e-1) - | (4.45e-1) - | (1.78e-1) - | (3.93e-1) - | **(4.59e-1)** |
| WFG4 | 3 | 1.3245e-1 | 1.7559e-1 | 1.9455e-1 | 8.4217e-2 | 1.7593e-1 | 1.0044e-1 | 8.4244e-2 | 2.5721e-1 | 1.6710e-1 | **8.0358e-2** |
| | | (7.25e-3) - | (5.50e-3) - | (1.04e-2) - | (2.27e-3) - | (4.04e-3) - | (3.88e-3) - | (1.73e-3) - | (2.52e-2) - | (7.19e-3) - | **(2.01e-3)** |
| | 5 | 5.4072e-1 | 1.0925e+0 | 7.6049e-1 | 4.4243e-1 | 5.7422e-1 | 4.4411e-1 | 4.3898e-1 | 8.3483e-1 | 6.3569e-1 | **3.4915e-1** |
| | | (2.11e-2) - | (1.46e-1) - | (7.32e-2) - | (1.10e-2) - | (1.56e-2) - | (9.76e-3) - | (8.21e-3) - | (6.62e-2) - | (2.10e-2) - | **(5.67e-3)** |
| | 10 | 1.6306e+0 | 8.9976e+0 | 2.2889e+0 | 1.0555e+0 | 1.4486e+0 | 1.1303e+0 | 1.1150e+0 | 2.1200e+0 | 1.4171e+0 | **1.0075e+0** |
| | | (2.25e-1) - | (6.30e-1) - | (4.23e-1) - | (1.43e-2) - | (1.41e-1) - | (7.20e-2) - | (2.99e-2) - | (2.18e-1) - | (1.83e-2) - | **(7.67e-3)** |
| | 15 | 2.5956e+0 | 2.0439e+1 | 8.7836e+0 | 3.9096e+0 | 1.7437e+0 | 4.6259e+0 | 3.6372e+0 | 2.4872e+0 | 3.6024e+0 | **1.5511e+0** |
| | | (6.83e-1) - | (7.52e-1) - | (4.81e+0) - | (6.26e-1) - | (2.72e-1) - | (1.52e+0) - | (1.05e+0) - | (2.31e-1) - | (6.46e-1) - | **(1.66e-2)** |
| WFG5 | 3 | 1.4799e-1 | 2.0761e-1 | 1.8176e-1 | 1.3358e-1 | 1.6577e-1 | 1.3827e-1 | 1.3535e-1 | 1.9671e-1 | 1.7712e-1 | **1.2743e-1** |
| | | (3.37e-3) - | (1.24e-2) - | (6.74e-3) - | (1.19e-3) - | (4.95e-3) - | (1.61e-3) - | (1.19e-3) - | (2.96e-2) - | (1.22e-2) - | **(1.14e-3)** |
| | 5 | 5.3319e-1 | 8.8219e-1 | 1.0866e+0 | 4.7123e-1 | 6.6531e-1 | 4.6520e-1 | 4.7146e-1 | 7.7145e-1 | 1.0304e+0 | **3.9619e-1** |
| | | (2.24e-2) - | (9.06e-2) - | (1.59e-1) - | (8.11e-3) - | (4.56e-2) - | (5.55e-3) - | (5.89e-3) - | (8.99e-2) - | (2.17e-1) - | **(4.95e-3)** |
| | 10 | 1.6394e+0 | 8.3133e+0 | 4.3615e+0 | 1.1032e+0 | 2.3787e+0 | 1.1825e+0 | 1.1739e+0 | 3.0437e+0 | 3.2953e+0 | **1.0593e+0** |
| | | (1.93e-1) - | (7.95e-1) - | (6.14e-1) - | (1.25e-2) - | (3.55e-1) - | (1.49e-2) - | (2.61e-2) - | (3.95e-1) - | (1.70e-1) - | **(5.98e-3)** |
| | 15 | 2.6559e+0 | 1.9414e+1 | 1.5313e+1 | 3.2419e+0 | 8.0861e+0 | 2.0227e+0 | 2.7743e+0 | 7.5746e+0 | 4.1034e+0 | **1.5830e+0** |
| | | (6.14e-1) - | (1.19e+0) - | (2.11e+0) - | (4.05e-1) - | (4.94e+0) - | (3.88e-1) - | (4.82e-1) - | (2.46e+0) - | (2.30e-1) - | **(1.44e-2)** |
| WFG6 | 3 | 1.6216e-1 | 2.4977e-1 | 2.3965e-1 | 1.5638e-1 | 1.5579e-1 | 1.7076e-1 | 1.5692e-1 | 3.0617e-1 | 1.8727e-1 | **1.6295e-1** |
| | | (4.19e-2) = | (2.37e-2) - | (4.86e-2) - | (1.57e-2) = | (2.86e-2) = | (2.36e-2) = | (2.13e-2) = | (3.88e-2) - | (1.62e-2) - | **(1.97e-2)** |
| | 5 | 6.3651e-1 | 1.1773e+0 | 8.2360e-1 | 5.2659e-1 | 7.5727e-1 | 5.1031e-1 | 5.1869e-1 | 7.5148e-1 | 8.3768e-1 | **4.4253e-1** |
| | | (5.43e-2) - | (1.70e-1) - | (1.08e-1) - | (2.23e-2) - | (2.33e-2) - | (3.37e-2) - | (2.20e-2) - | (2.66e-2) - | (6.83e-2) - | **(2.07e-2)** |
| | 10 | 1.7116e+0 | 8.4410e+0 | 2.5207e+0 | 1.1294e+0 | 1.5652e+0 | 1.1860e+0 | 1.1654e+0 | 1.6376e+0 | 1.9043e+0 | **1.1109e+0** |
| | | (1.94e-1) - | (8.17e-1) - | (8.38e-1) - | (3.55e-2) - | (6.17e-2) - | (3.45e-2) - | (2.98e-2) - | (1.15e-1) - | (4.67e-1) - | **(1.94e-2)** |
| | 15 | 2.6708e+0 | 1.9528e+1 | 1.4962e+1 | 3.3104e+0 | 3.3009e+0 | 2.1622e+0 | 3.2406e+0 | 1.8233e+0 | 4.0088e+0 | **1.6243e+0** |
| | | (6.37e-1) - | (1.19e+0) - | (3.32e+0) - | (4.43e-1) - | (4.18e+0) - | (7.92e-1) - | (8.21e-1) - | (3.98e-2) - | (7.45e-1) - | **(2.72e-2)** |
| WFG7 | 3 | 1.1328e-1 | 1.8771e-1 | 1.6507e-1 | **7.8473e-2** | 2.2692e-1 | 9.6361e-2 | 8.1865e-2 | 3.3261e-1 | 1.5629e-1 | 8.1236e-2 |
| | | (4.42e-3) - | (6.11e-3) - | (1.44e-2) - | **(1.30e-3)+** | (2.27e-2) - | (2.60e-3) - | (1.77e-3) = | (3.50e-2) - | (1.10e-2) - | (1.64e-3) |
| | 5 | 5.2618e-1 | 1.0244e+0 | 1.0160e+0 | 4.1016e-1 | 7.2307e-1 | 4.4090e-1 | 4.1374e-1 | 9.9196e-1 | 6.8775e-1 | **3.4668e-1** |
| | | (2.69e-2) - | (1.36e-1) - | (1.42e-1) - | (1.25e-2) - | (1.67e-2) - | (1.28e-2) - | (9.90e-3) - | (9.01e-2) - | (4.91e-2) - | **(5.84e-3)** |
| | 10 | 1.4834e+0 | 8.4211e+0 | 4.3782e+0 | 1.0477e+0 | 1.5836e+0 | 1.2046e+0 | 1.1240e+0 | 2.6007e+0 | 2.1363e+0 | **1.0085e+0** |
| | | (1.38e-1) - | (6.47e-1) - | (8.28e-1) - | (2.19e-2) - | (6.46e-2) - | (8.03e-2) - | (1.15e-1) - | (1.58e-1) - | (6.20e-1) - | **(8.85e-3)** |
| | 15 | 2.2446e+0 | 1.9574e+1 | 1.7617e+1 | 5.2529e+0 | 4.5265e+0 | 3.4012e+0 | 5.4035e+0 | 2.8696e+0 | 3.4652e+0 | **1.5392e+0** |
| | | (6.01e-1) - | (1.28e+0) - | (1.59e+0) - | (5.83e-1) - | (3.66e+0) - | (1.12e+0) - | (9.03e-1) - | (1.62e-1) - | (2.83e-1) - | **(1.52e-2)** |
| +/ − / = | | 1/26/1 | 2/26/0 | 0/28/0 | 6/20/2 | 2/22/4 | 2/22/4 | 2/23/3 | 0/28/0 | 1/26/1 | |

**Table 6.** IGD+ values on MaF test problems.

| Problem | M | IGD+ | | | | | | | | | |
|---|---|---|---|---|---|---|---|---|---|---|---|
| | | CMOEA-CD | IMC-MOEAD | LERD | NRVMOEA | FDV | HEA | LMPFE | DGEA | NSGAII-ARSBX | DES-NSGA-II |
| MaF1 | 3 | 4.2566e-2 | 8.5393e-2 | 6.5735e-2 | **3.1083e-2** | 6.3112e-2 | 5.3280e-2 | 3.4404e-2 | 1.0356e-1 | 4.8618e-2 | 3.3654e-2 |
| | | (2.15e-3) - | (1.01e-2) - | (3.57e-3) - | **(2.88e-4)+** | (1.88e-3) - | (9.03e-4) - | (7.91e-4) - | (1.04e-2) - | (2.74e-3) - | (8.63e-4) |
| | 5 | 1.5039e-1 | 1.6429e-1 | 2.0373e-1 | **9.7519e-2** | 2.8377e-1 | 1.4870e-1 | 1.0069e-1 | 3.7139e-1 | 1.4594e-1 | 1.0774e-1 |
| | | (1.01e-2) - | (1.13e-2) - | (1.06e-2) - | **(1.97e-3)+** | (2.26e-2) - | (4.56e-3) - | (2.96e-3)+ | (4.45e-2) - | (8.04e-3) - | (1.73e-3) |
| | 10 | 3.1195e-1 | 2.9870e-1 | 3.3259e-1 | **1.9639e-1** | 4.1727e-1 | 2.5491e-1 | 2.0310e-1 | 4.8546e-1 | 2.4214e-1 | 2.4179e-1 |
| | | (1.74e-2) - | (2.09e-2) - | (1.77e-2) - | **(1.29e-2)+** | (2.18e-2) - | (1.35e-2) - | (3.06e-2)+ | (5.20e-2) - | (7.66e-3) = | (4.41e-3) |
| | 15 | 3.9372e-1 | 3.4950e-1 | 3.8704e-1 | 3.1615e-1 | 4.3754e-1 | 3.3397e-1 | **2.7084e-1** | 5.8304e-1 | 2.6805e-1 | 2.9698e-1 |
| | | (2.40e-2) - | (1.97e-2) - | (1.44e-2) - | (1.93e-2) - | (1.76e-2) - | (1.73e-2) - | **(2.12e-2)+** | (1.04e-1) - | (6.25e-3)+ | (2.88e-3) |
| MaF2 | 3 | 3.8244e-2 | 3.0520e-2 | 3.6739e-2 | **1.9037e-2** | 2.8451e-2 | 2.2443e-2 | 1.9321e-2 | 3.6188e-2 | 4.0211e-2 | 1.9624e-2 |
| | | (1.63e-3) - | (6.03e-4) - | (1.32e-3) - | **(1.74e-4)+** | (1.02e-3) - | (2.24e-4) - | (3.88e-4)+ | (3.27e-3) - | (3.11e-3) - | (6.75e-4) |
| | 5 | 9.2926e-2 | 9.3583e-2 | 1.3037e-1 | **6.1919e-2** | 1.1006e-1 | 8.1701e-2 | 6.6068e-2 | 9.8112e-2 | 1.0711e-1 | 6.8426e-2 |
| | | (3.26e-3) - | (2.01e-3) - | (5.68e-3) - | **(1.20e-3)+** | (3.11e-2) - | (1.83e-3) - | (2.42e-3)+ | (4.88e-3) - | (3.51e-3) - | (1.74e-3) |
| | 10 | 1.3159e-1 | 2.8334e-1 | 2.0501e-1 | **1.1261e-1** | 4.8027e-1 | 1.3973e-1 | 1.2434e-1 | 2.6851e-1 | 1.3445e-1 | 1.2441e-1 |
| | | (2.63e-3) - | (3.41e-2) - | (1.14e-2) - | **(3.36e-3)+** | (9.23e-3) - | (2.97e-3) - | (2.89e-2)+ | (7.08e-2) - | (2.66e-3) - | (5.18e-3) |
| | 15 | 1.3630e-1 | 3.6307e-1 | 3.9175e-1 | **1.2925e-1** | 5.0492e-1 | 1.6079e-1 | 1.6885e-1 | 4.0342e-1 | 1.2358e-1 | 1.8447e-1 |
| | | (2.72e-3)+ | (4.88e-2) - | (3.00e-2) - | **(6.63e-3)+** | (4.94e-3) - | (9.64e-3)+ | (1.91e-2)+ | (7.38e-2) - | (2.18e-3)+ | (2.08e-2) |
| MaF3 | 3 | 3.3848e-1 | 9.5238e+3 | 1.0903e+4 | 1.1864e+2 | **2.0668e-2** | 1.4110e+3 | 1.2462e+2 | 2.1312e+4 | 8.4003e+3 | 7.5395e-1 |
| | | (8.02e-1)+ | (6.07e+3) - | (1.45e+4) - | (1.22e+2) - | **(1.09e-3)+** | (4.11e+3) - | (1.61e+2) - | (1.63e+4) - | (4.97e+3) - | (1.72e+0) |
| | 5 | 1.5857e+1 | 1.5107e+4 | 1.8921e+6 | 5.7742e+3 | **9.3720e-2** | 3.2573e+3 | 2.5796e+3 | 2.0674e+4 | 5.0853e+4 | 1.9040e-1 |
| | | (2.05e+1) - | (1.45e+4) - | (1.03e+7) - | (5.26e+3) - | **(3.54e-1)+** | (6.75e+3) - | (2.32e+3) - | (1.74e+4) - | (2.92e+4) - | (4.81e-1) |
| | 10 | 3.1383e+2 | 5.4742e+5 | 4.5967e+6 | 2.0346e+9 | **2.1483e-1** | 1.4950e+3 | 1.2652e+6 | 2.4562e+4 | 2.2993e+8 | 3.4962e+0 |
| | | (6.53e+2) - | (1.28e+6) - | (2.51e+7) - | (2.64e+9) - | **(4.27e-1)=** | (5.44e+3) - | (9.45e+5) - | (1.66e+4) - | (1.21e+9) - | (9.30e+0) |
| | 15 | 3.7727e+3 | 4.5538e+6 | 1.0393e+8 | 2.0065e+9 | **2.0439e-1** | 2.4969e+3 | 1.8842e+5 | 1.3833e+4 | 4.4376e+6 | 2.8109e-1 |
| | | (8.97e+3) - | (1.41e+7) - | (2.69e+8) - | (2.87e+9) - | **(9.41e-2)=** | (1.26e+4) - | (8.60e+4) - | (1.56e+4) - | (6.55e+6) - | (2.58e-1) |
| MaF4 | 3 | 1.1246e+0 | 1.5851e+2 | 6.2636e+1 | 2.3053e+1 | **1.8208e-1** | 1.7672e+1 | 2.0065e+1 | 3.7799e+2 | 3.0455e+2 | 7.3488e-1 |
| | | (1.88e+0) = | (4.21e+1) - | (6.98e+1) - | (1.60e+1) - | **(1.18e-2)+** | (9.70e+0) - | (9.20e+0) - | (1.85e+2) - | (7.90e+1) - | (1.13e+0) |
| | 5 | 1.7156e+1 | 6.4314e+2 | 7.1771e+2 | 1.8519e+2 | **1.8692e+0** | 9.1263e+1 | 4.3121e+2 | 1.0672e+3 | 1.6231e+3 | 1.9226e+0 |
| | | (2.26e+1) - | (2.10e+2) - | (5.46e+2) - | (8.87e+1) - | **(1.91e-1) -** | (7.81e+1) - | (1.55e+3) - | (5.95e+2) - | (3.67e+2) - | (2.76e-1) |
| | 10 | 1.1550e+3 | 2.4165e+4 | 2.4994e+4 | 4.5049e+2 | **4.0789e+1** | 3.5726e+3 | 1.9238e+3 | 4.3249e+4 | 6.9150e+4 | 6.9801e+1 |
| | | (1.01e+3) - | (9.30e+3) - | (1.79e+4) - | (2.23e+3) - | **(2.67e+0)+** | (3.25e+3) - | (6.79e+3) - | (2.64e+4) - | (1.91e+4) - | (1.27e+1) |
| | 15 | 8.8366e+3 | 8.3571e+5 | 1.1916e+6 | 2.2209e+5 | 9.8887e+2 | 1.8180e+5 | 2.0465e+5 | 1.5671e+6 | 1.4688e+5 | **9.9833e+2** |
| | | (1.68e+4) - | (4.16e+5) - | (7.02e+5) - | (1.34e+5) - | (3.13e+2) - | (1.28e+5) - | (1.56e+5) - | (1.17e+6) - | (9.40e+4) - | **(2.08e+2)** |
| MaF5 | 3 | **9.5955e-2** | 2.8144e-1 | 7.6708e-1 | 5.0476e-1 | 2.1525e-1 | 8.2643e-1 | 4.5666e-1 | 4.6496e-1 | 1.3639e-1 | 3.1160e-1 |
| | | **(5.82e-3)+** | (9.96e-2)+ | (1.89e+0) - | (7.99e-1) - | (9.44e-2)+ | (1.20e+0) - | (7.85e-1) - | (2.59e-1) - | (5.18e-3) - | (7.66e-1) |
| | 5 | 5.7151e-1 | 1.5084e+0 | 8.3242e-1 | 4.6517e-1 | 8.9209e-1 | 7.5748e-1 | 6.3903e-1 | 1.3828e+0 | 1.0565e+0 | **4.2781e-1** |
| | | (2.95e-2) - | (3.70e-1) - | (2.13e-1) - | (5.52e-2) - | (5.91e-2) - | (5.56e-1) - | (1.00e-1) - | (2.54e-1) - | (7.33e-2) - | **(6.56e-2)** |
| | 10 | 3.0100e+0 | 3.9881e+2 | 1.6253e+0 | 1.1358e+0 | 1.4615e+0 | 1.3223e+0 | 7.2656e+4 | 2.2495e+0 | 3.8424e+0 | **1.1165e+2** |
| | | (6.85e+0) - | (2.88e+2) - | (1.77e-1) - | (1.77e-2) - | (2.99e-2) - | (2.25e-1) - | (3.73e+5) - | (5.29e-1) - | (8.35e-1) - | **(1.66e-2)** |
| | 15 | 3.2034e+0 | 1.6249e+4 | 2.2593e+0 | **1.5121e+0** | 1.6492e+0 | 3.6457e+0 | 2.4520e+0 | 2.2743e+0 | 5.0369e+0 | 1.5906e+0 |
| | | (3.64e+0) - | (8.96e+3) - | (3.83e-1) - | **(9.48e-2)+** | (3.66e-2) - | (3.17e+0) - | (6.18e-1) - | (4.47e-1) - | (6.69e-1) - | (1.58e-2) |
| MaF6 | 3 | **1.8139e-3** | 2.4919e-1 | 1.1307e-2 | 4.1646e-3 | 1.4371e-2 | 1.7636e-2 | 4.3574e-3 | 7.2264e-2 | 2.7983e-3 | 2.8784e-3 |
| | | **(3.09e-5)+** | (6.25e-2) - | (7.57e-4) - | (1.03e-3) - | (4.62e-4) - | (2.15e-3) - | (4.82e-3) - | (2.71e-2) - | (1.67e-4) = | (3.37e-4) |
| | 5 | **1.8440e-3** | 2.9962e-1 | 6.8232e-2 | 3.8090e-3 | 3.2654e-2 | 2.4680e-2 | 5.0138e-3 | 8.9077e-2 | 3.0239e-3 | 4.2019e-3 |
| | | **(3.12e-5)+** | (9.50e-2) - | (4.57e-2) - | (6.54e-4) = | (1.57e-4) - | (1.51e-3) - | (5.43e-3) - | (4.09e-2) - | (2.76e-4)+ | (7.84e-4) |
| | 10 | 1.4130e-1 | 9.6879e-1 | 2.1502e-1 | 5.7844e-1 | 3.0586e-1 | 6.6313e-1 | 6.2996e-1 | 1.0078e-1 | 5.2717e+0 | **8.1897e-2** |
| | | (1.15e-1) - | (7.16e-1) - | (8.26e-4) - | (4.72e-1) - | (1.36e-1) - | (8.33e-1) = | (1.29e+0) = | (6.71e-2) = | (2.87e+0)+ | **(4.02e-2)** |
| | 15 | 1.2049e-1 | 8.2905e-1 | 2.2679e-1 | 8.5667e+0 | 3.6717e-1 | 3.7958e-1 | 4.8665e+0 | 3.5006e-1 | 3.9693e-1 | **1.0039e-1** |
| | | (8.23e-2) - | (9.58e-1) - | (3.49e-2) - | (4.80e+0) - | (3.34e-2) - | (1.32e+0) = | (2.47e+0) - | (2.62e-1) - | (2.19e-1) - | **(5.49e-2)** |
| MaF7 | 3 | **3.1268e-2** | 1.6079e-1 | 6.6350e-1 | 7.6305e-2 | 5.2809e-1 | 9.0704e-2 | 1.4538e-1 | 2.4345e+0 | 5.7357e-2 | 4.4284e-2 |
| | | **(7.83e-4) =** | (4.41e-2) - | (7.58e-2) - | (8.00e-2) - | (1.96e-1) - | (1.43e-1) - | (1.67e-1) - | (1.53e+0) - | (3.97e-3) - | (4.92e-2) |
| | 5 | 2.1868e-1 | 8.6025e-1 | 1.1376e+0 | 1.9733e-1 | 8.0707e-1 | 1.1101e+0 | 1.0599e+0 | 1.2949e+0 | 1.2147e+0 | **1.5095e-1** |
| | | (1.59e-2) - | (1.98e-1) - | (4.31e-1) - | (6.89e-2) - | (2.40e-1) - | (9.08e-1) - | (4.04e-1) - | (7.96e-1) - | (2.90e-1) - | **(7.92e-3)** |
| | 10 | 1.5510e+0 | 2.0590e+1 | 5.5555e+0 | **5.4424e-1** | 1.5092e+0 | 5.6803e+0 | 1.9063e+0 | 1.5866e+0 | 3.6137e+0 | 8.4315e-1 |
| | | (1.80e-1) - | (4.19e+0) - | (1.06e+0) - | **(1.36e-2)+** | (5.98e-1) - | (9.51e-1) - | (2.39e+0) - | (4.83e-1) - | (2.14e+0) - | (1.17e-1) |
| | 15 | 4.6564e+0 | 2.5607e+1 | 1.4840e+1 | 1.4445e+1 | **2.9283e+0** | 1.1851e+1 | 3.3656e+1 | 3.1029e+0 | 3.2458e+0 | 5.3349e+0 |
| | | (1.08e+0)+ | (5.21e+0) - | (4.88e+0) - | (2.00e+0) - | **(1.14e+0)+** | (4.96e-4) - | (5.13e+0) - | (1.13e+0)+ | (1.83e+0)+ | (3.39e-1) |
| +/ − / = | | 6/20/2 | 1/27/0 | 0/28/0 | 9/18/1 | 6/18/4 | 1/25/2 | 7/20/1 | 1/26/1 | 5/21/2 | |

**Table 7.** Average Friedman ranks and Holm-adjusted post-hoc results for IGD over $N = 84$ blocks and $k = 10$ algorithms. Rank 1 is best. The overall rank is the average over all 84 blocks. $p_{\text{Holm}}$ corresponds to DES-NSGA-II versus each competitor after Holm correction for nine comparisons, using the average-rank normal approximation of Demšar [36]. Values below $10^{-15}$ are reported as $< 10^{-15}$, which is far below any conventional significance threshold.

| Algorithm | DTLZ rank | WFG rank | MaF rank | Overall rank | $p_{\text{Holm}}$ vs DES |
|---|---|---|---|---|---|
| DES-NSGA-II | 1.607 | 1.821 | 2.357 | **1.929** | – |
| CMOEA-CD | 3.786 | 3.571 | 3.250 | 3.536 | $1.0 \times 10^{-3}$ |
| IMC-MOEAD | 8.000 | 8.464 | 7.786 | 8.083 | $< 10^{-15}$ |
| LERD | 6.571 | 8.679 | 7.643 | 7.631 | $< 10^{-15}$ |
| NRVMOEA | 4.107 | 3.857 | 4.357 | 4.107 | $6.2 \times 10^{-6}$ |
| FDV | 5.179 | 6.750 | 5.393 | 5.774 | $1.1 \times 10^{-15}$ |
| HEA | 5.464 | 4.714 | 5.714 | 5.298 | $2.2 \times 10^{-12}$ |
| LMPFE | 5.679 | 3.464 | 5.214 | 4.786 | $2.9 \times 10^{-9}$ |
| DGEA | 6.893 | 8.000 | 7.714 | 7.536 | $< 10^{-15}$ |
| NSGAII-ARSBX | 7.714 | 5.679 | 5.571 | 6.321 | $< 10^{-15}$ |
| Friedman omnibus test: $Q = 322.681$, df= 9, $p < 10^{-50}$; Kendall's $W = 0.4268$. | | | | | |

The clearest exception is DTLZ4 with $M = 3$, where the highly non-uniform point density induced by its $\alpha = 100$ mapping weakens selection rules that rely mainly on directional coverage. On this instance, CMOEA-CD and NSGAII-ARSBX attain $5.59 \times 10^{-2}$ and $6.87 \times 10^{-2}$ in IGD, against $1.80 \times 10^{-1}$ for DES-NSGA-II. The gap widens in IGD$^+$, where CMOEA-CD ($2.60 \times 10^{-2}$), NSGAII-ARSBX ($3.77 \times 10^{-2}$) and FDV ($7.26 \times 10^{-2}$) all fall below the $7.57 \times 10^{-2}$ obtained by DES-NSGA-II. This behavior is consistent with the convergence–diversity conflict of DTLZ4, on which the second selection stage is forced to trade convergence for angular coverage earlier than on the remaining DTLZ problems. At $M = 15$, NRVMOEA is the best algorithm on DTLZ7, while DES-NSGA-II remains competitive on DTLZ1 and DTLZ6. On WFG, DES-NSGA-II attains the best average rank (1.821), while LMPFE and NRVMOEA are stronger on individual WFG1 and WFG2 instances. On MaF, DES-NSGA-II again attains the best average rank (2.357), followed by CMOEA-CD (3.250) and NRVMOEA (4.357); FDV, which is the strongest method on the disconnected MaF3 front, ranks fifth on the suite as a whole (5.393), since its advantage does not extend to the remaining MaF instances. The MaF margin is therefore narrower than that on DTLZ and WFG.

These results are consistent with the design of the proposed method. Rather than imposing a fixed selection pressure throughout the evolutionary process, DES-NSGA-II modulates it according to the perceived population state (Section 2.6) and applies it only during the diversity-enhancement stage, so that on the regular DTLZ and WFG fronts the pressure stays high enough to preserve convergence while the second stage broadens the directional distribution. On the irregular and disconnected fronts the same mechanism is insufficient because the pressure signal does not carry the connectivity information that FDV exploits explicitly; this is where the margin is lost, and it motivates future work on adapting $S_1$ to front connectivity.

Figures 2 and 3 complement this mean-based account with the run-to-run distribution and with the evolution of the indicators over the search.

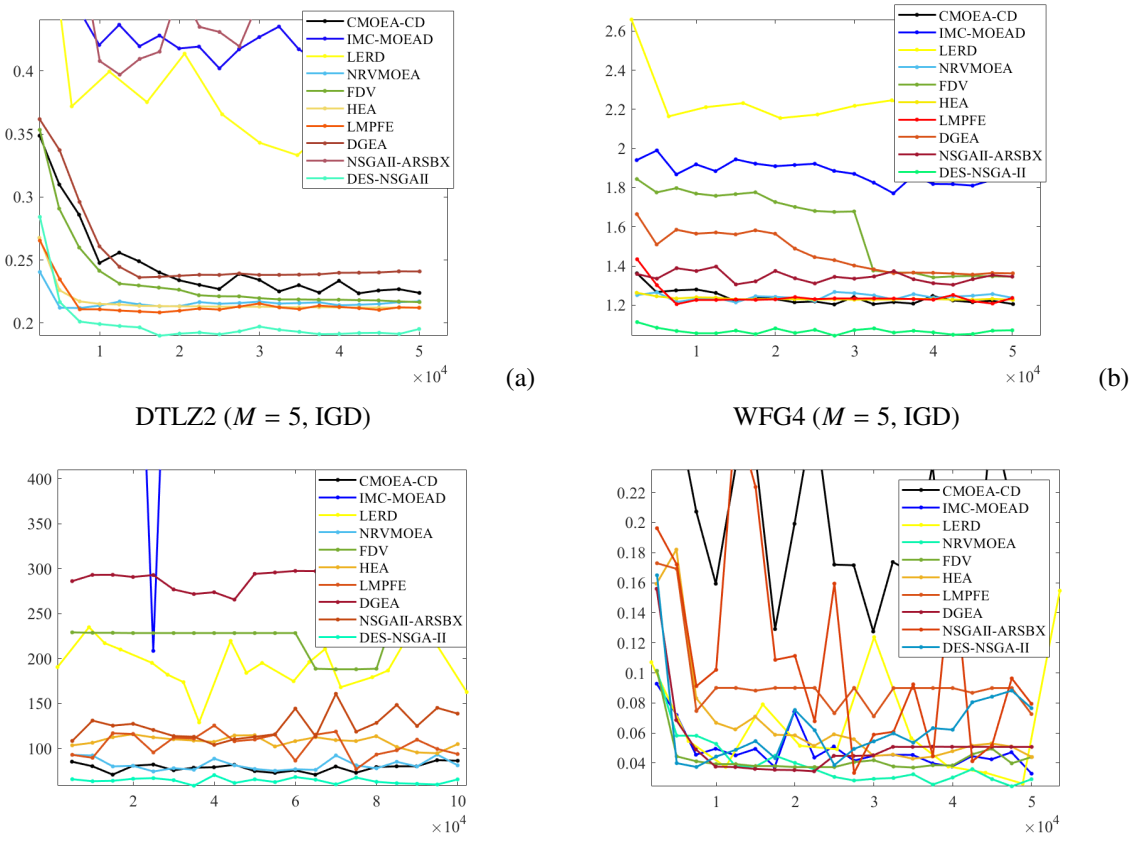


**Figure 3.** Convergence trajectories of the IGD and IGD$^+$ indicators on representative test problems. The horizontal axis denotes the number of function evaluations, and the vertical axis denotes the indicator value.

Run-to-run stability

To complement the mean-based comparison, Figure 2 reports boxplots of IGD over 30 independent runs on three representative instances with different Pareto-front geometries. A lower median indicates better convergence, whereas a narrower box and shorter whiskers indicate more stable run-to-run performance. On DTLZ1 ($M = 10$) and WFG4 ($M = 10$), DES-NSGA-II shows a substantially lower median IGD and a remarkably smaller interquartile range than all competing algorithms, demonstrating superior convergence and robustness. On MaF3 ($M = 10$), FDV remains the strongest, and the boxplots confirm that DES-NSGA-II does not attain the best median IGD on this instance. These boxplots are descriptive; the formal significance conclusions are based on the Wilcoxon and Friedman tests reported in Table 7 and the main result tables.

### *3.3. Convergence trajectories*

To further examine the convergence behavior of DES-NSGA-II, Figure 3 tracks the evolution of the IGD and IGD$^+$ indicators over the course of the optimization process on four representative instances: DTLZ2 with $M = 5$, WFG4 with $M = 5$, MaF5 with $M = 10$, and DTLZ5 with $M = 5$ (IGD$^+$).

Figure 3 illustrates the convergence trajectories of IGD and IGD$^+$. On DTLZ2 (a) and WFG4 (b),

DES-NSGA-II achieves the fastest initial descent and maintains the lowest indicator values throughout the search, clearly outperforming LERD and IMC-MOEAD. On the high-dimensional MaF5 (c), DES-NSGA-II remains highly stable, avoiding the severe stagnation or fluctuations exhibited by several competitors. For DTLZ5 with IGD$^+$ (d), the gap is narrower, yet DES-NSGA-II converges to the lowest tier alongside NRVMOEA while avoiding the large oscillations of CMOEA-CD. Overall, these trajectories confirm that the proposed mechanism not only accelerates the convergence speed but also improves final solution quality, especially in high-dimensional spaces.

Statistical superiority

Table 7 reports the average Friedman ranks, Kendall's $W$, and Holm-adjusted pairwise results for IGD over $N = 84$ blocks. DES-NSGA-II obtains the best overall average rank (1.929), followed by CMOEA-CD (3.536). The Holm-adjusted values are computed from the average-rank normal approximation of Demšar [36] and are distinct from the per-instance Wilcoxon counts at the bottom of Tables 1–6: the former tests average-rank differences over all blocks, whereas the latter counts per-instance wins, ties, and losses. After Holm correction, all nine comparisons remain significant at $\alpha = 0.05$; the smallest margin is against CMOEA-CD ($p_{\text{Holm}} = 1.0 \times 10^{-3}$), and the remaining eight are significant at $p_{\text{Holm}} < 10^{-5}$.

### *3.4. Evolution of the adaptive selection pressure*

To empirically examine the dynamic behavior of the proposed regulation model, the evolution of $\beta_t$, together with the population-state signals $S_1$ and $S_2$, is recorded during the optimization process. DTLZ1 with $M = 10$ objectives is selected as a representative case, and the corresponding trajectories are shown in Figure 4.

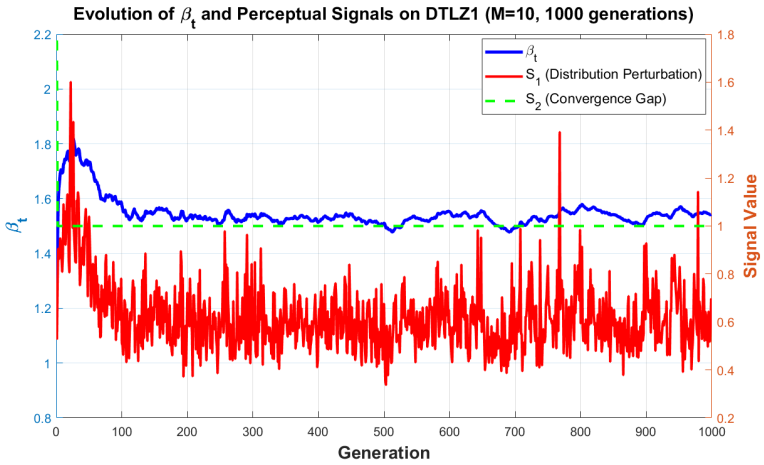


**Figure 4.** Evolutionary trajectories of $\beta_t$ and the population-state signals on DTLZ1 ($M = 10$).

As shown in Figure 4, $\beta_t$ remains within approximately 1.25–1.82, fully satisfying the theoretical bound

$$1 \leq \beta_t < 2. \tag{3.3}$$

During the early evolutionary stage ($t < 50$), $\beta_t$ increases from approximately 1.25 to 1.81, after which it gradually decreases and stabilizes around 1.45. In the later stage ($t \geq 300$), the intergenerational variation of $\beta_t$ remains below approximately 0.05, indicating that the temporal smoothing mechanism effectively attenuates short-term fluctuations.

The evolution of $\beta_t$ is broadly consistent with that of $S_1$. Specifically, $S_1$ decreases from approximately 1.30 in the early stage to around 1.00 toward the end, accompanied by a corresponding decrease in $\beta_t$. This trend is consistent with the monotonic dependence of the regulation model on $S_1$. However, $\beta_t$ is jointly determined by $S_1$, $S_2$, the nonlinear mapping, and temporal smoothing, and therefore should not be interpreted as being controlled by $S_1$ alone.

The convergence-discrepancy signal $S_2$ varies within approximately 1.000–1.327. It increases during the early stage and subsequently fluctuates within a relatively moderate range, providing additional state information for adaptive pressure regulation. Compared with $S_1$, its variation is smaller in this experiment. Since the current formulation uses

$$\beta_t^{\text{raw}} = S_{1,t} S_{2,t}^{\alpha_t}, \tag{3.4}$$

an increase in $S_{2,t}$ contributes positively to the raw selection pressure when $S_{1,t} > 0$. Overall, the observed trajectories demonstrate that the proposed controller maintains the theoretical bound while adapting the selection pressure to the evolving population state.

### *3.5. Ablation study*

To investigate the contributions of the core components of the proposed DES-NSGA-II, ablation experiments were conducted on three representative problems: DTLZ2 (regular), WFG4 (complex mixed), and MaF3 (disconnected). Six configurations were compared: Full, Fixed $\beta$, Single-stage, w/o $S_1$, w/o $S_2$, and LinearDecay. Fixed $\beta$ replaces the adaptive pressure with a constant $\beta = 1.5$. Single-stage removes the second selection stage. The w/o $S_1$ and w/o $S_2$ variants fix $S_{1,t} = 1$ and $S_{2,t} = 1$, respectively. LinearDecay uses a predetermined strategy

$$\beta_t = \max\{\beta_{\min}, \beta_0 - (\beta_0 - \beta_{\min})t/T\}$$

with $\beta_0 = 1.5$ and $\beta_{\min} = 1.0$.

The `w/oS1` variant fixes $S_{1,t} \equiv 1$ (i.e., removes the IQR-based dispersion feedback), while the `w/oS2` variant fixes $S_{2,t} \equiv 1$ (i.e., removes the relative convergence-discrepancy feedback). In both variants, $\beta_t$ is recomputed from the remaining signal and still passes through the same tanh bounding and temporal-smoothing pipeline.

All configurations use the exact same settings as the main comparison ($N = 100$, maxFE = $M \times 10^4$, same paired seeds). Consequently, the Full row matches the main result tables identically. The mean IGD and the relative change are reported in Tables 8–10, where percentages in parentheses indicate relative changes to Full (positive means worse performance). Due to space limitations, Tables 8–10 report IGD only.

**Table 8.** Ablation study: mean IGD on DTLZ2 (30 runs).

| $M$ | Full | Fixed $\beta$ | Single-stage | w/o $S_1$ | w/o $S_2$ | LinearDecay |
|---|---|---|---|---|---|---|
| 3 | $4.87 \times 10^{-2}$ | $3.62 \times 10^{-2}$ | $4.87 \times 10^{-2}$ | $4.85 \times 10^{-2}$ | $5.49 \times 10^{-2}$ | $4.17 \times 10^{-2}$ |
| | | (−25.7%) | (0.0%) | (−0.5%) | (+12.9%) | (−14.3%) |
| 5 | $1.93 \times 10^{-1}$ | $2.09 \times 10^{-1}$ | $2.33 \times 10^{-1}$ | $1.93 \times 10^{-1}$ | $2.02 \times 10^{-1}$ | $1.88 \times 10^{-1}$ |
| | | (+8.5%) | (+21.2%) | (0.0%) | (+5.1%) | (−2.5%) |
| 10 | $4.56 \times 10^{-1}$ | $5.14 \times 10^{-1}$ | $5.41 \times 10^{-1}$ | $4.53 \times 10^{-1}$ | $4.65 \times 10^{-1}$ | $4.52 \times 10^{-1}$ |
| | | (+12.7%) | (+18.5%) | (−0.8%) | (+2.0%) | (−1.0%) |
| 15 | $5.79 \times 10^{-1}$ | $6.19 \times 10^{-1}$ | $6.33 \times 10^{-1}$ | $5.62 \times 10^{-1}$ | $5.78 \times 10^{-1}$ | $5.64 \times 10^{-1}$ |
| | | (+6.8%) | (+9.3%) | (−3.0%) | (−0.3%) | (−2.6%) |

**Table 9.** Ablation study: mean IGD on WFG4 (30 runs).

| $M$ | Full | Fixed $\beta$ | Single-stage | w/o $S_1$ | w/o $S_2$ | LinearDecay |
|---|---|---|---|---|---|---|
| 3 | $1.96 \times 10^{-1}$ | $1.91 \times 10^{-1}$ | $1.94 \times 10^{-1}$ | $1.89 \times 10^{-1}$ | $1.93 \times 10^{-1}$ | $1.94 \times 10^{-1}$ |
| | | (−2.5%) | (−1.3%) | (−3.8%) | (−1.9%) | (−1.3%) |
| 5 | $1.06 \times 10^{0}$ | $1.05 \times 10^{0}$ | $1.02 \times 10^{0}$ | $1.04 \times 10^{0}$ | $1.05 \times 10^{0}$ | $1.06 \times 10^{0}$ |
| | | (−1.0%) | (−4.0%) | (−2.5%) | (−1.5%) | (0.0%) |
| 10 | $4.81 \times 10^{0}$ | $4.94 \times 10^{0}$ | $5.17 \times 10^{0}$ | $4.73 \times 10^{0}$ | $4.77 \times 10^{0}$ | $4.75 \times 10^{0}$ |
| | | (+2.6%) | (+7.4%) | (−1.7%) | (−0.9%) | (−1.3%) |
| 15 | $8.59 \times 10^{0}$ | $8.64 \times 10^{0}$ | $1.56 \times 10^{1}$ | $8.25 \times 10^{0}$ | $8.68 \times 10^{0}$ | $8.15 \times 10^{0}$ |
| | | (+0.6%) | (+81.7%) | (−4.0%) | (+1.1%) | (−5.2%) |

**Table 10.** Ablation study: mean IGD on MaF3 (30 runs).

| $M$ | Full | Fixed $\beta$ | Single-stage | w/o $S_1$ | w/o $S_2$ | LinearDecay |
|---|---|---|---|---|---|---|
| 3 | $8.57 \times 10^{-1}$ | $3.75 \times 10^{-1}$ | $2.50 \times 10^{-1}$ | $8.98 \times 10^{-1}$ | $7.92 \times 10^{-1}$ | $1.85 \times 10^{0}$ |
| | | (−56.3%) | (−70.9%) | (+4.7%) | (−7.6%) | (+115.8%) |
| 5 | $2.84 \times 10^{-1}$ | $4.26 \times 10^{-1}$ | $7.65 \times 10^{-1}$ | $2.80 \times 10^{-1}$ | $3.00 \times 10^{-1}$ | $2.80 \times 10^{-1}$ |
| | | (+50.0%) | (+169.3%) | (−1.4%) | (+5.7%) | (−1.4%) |
| 10 | $3.57 \times 10^{0}$ | $3.27 \times 10^{0}$ | $1.99 \times 10^{1}$ | $5.04 \times 10^{0}$ | $3.39 \times 10^{0}$ | $6.14 \times 10^{0}$ |
| | | (−8.5%) | (+457.8%) | (+41.2%) | (−5.0%) | (+71.9%) |
| 15 | $3.44 \times 10^{-1}$ | $5.64 \times 10^{-1}$ | $1.25 \times 10^{0}$ | $4.72 \times 10^{-1}$ | $1.01 \times 10^{0}$ | $3.84 \times 10^{-1}$ |
| | | (+64.1%) | (+263.7%) | (+37.4%) | (+193.5%) | (+11.8%) |

Note: Full denotes the complete DES-NSGA-II. Fixed $\beta$ removes adaptive pressure regulation; Single-stage removes the two-stage hierarchical selection; w/o $S_1$ and w/o $S_2$ remove the corresponding state-perception signals. Percentages indicate the performance change relative to Full.

The results reveal structure-dependent patterns. On the regular DTLZ2 front, simplified variants remain competitive; Fixed $\beta$ reduces IGD by 25.7% at $M = 3$, and w/o $S_1$ is slightly better at $M = 15$ (a 3.0% reduction). However, on the complex MaF3 and WFG4 fronts, the complete two-stage mechanism becomes essential at higher dimensions. For instance, removing the second stage (Single-stage) causes severe degradation at $M = 10$ and $M = 15$ on MaF3 (increases of 457.8% and 263.7%), and an 81.7% increase at $M = 15$ on WFG4. These observations indicate that while Fixed $\beta$ is a strong

baseline for low-dimensional regular problems, the adaptive two-stage niching is crucial to prevent performance collapse on complex, high-dimensional fronts.

**Sensitivity of the prioritization factor.** To examine whether the prioritization order in Eq (2.35) is sensitive to the constant factor, we varied the factor over $\{1, 2, 3\}$ on DTLZ2 and WFG4 with $M = 10$ (30 runs each, paired random seeds). The average IGD changes by up to 36.63% relative to the default setting: DTLZ2 favors $\lambda = 1$ (a decrease of 30.04% in IGD), whereas WFG4 slightly favors the default $\lambda = 2$ (increases of 21.96% and 18.21% for $\lambda = 1$ and $\lambda = 3$, respectively). Due to the large variance across independent runs on these landscapes, the paired Wilcoxon signed-rank tests find no statistically significant difference between the configurations (all $p > 0.38$). Since no single factor uniformly dominates across different Pareto-front structures, $\lambda = 2$ is retained as a deterministic setting to avoid introducing an additional tuned parameter.

## 4. Conclusions and future work

This paper proposed DES-NSGA-II, a dynamic environmental-selection strategy developed within the NSGA-II framework for many-objective optimization. The proposed method establishes a closed-loop mechanism that integrates robust population-state perception, adaptive selection-pressure regulation, and two-stage hierarchical niching. Two statistical indicators are employed to characterize distributional disturbance and convergence discrepancy, respectively, and their joint information is transformed into an adaptive selection-pressure coefficient. The first stage of environmental selection constructs a convergence-oriented population skeleton, while the second stage enhances directional diversity under the regulation of the adaptive selection pressure. This design enables the environmental-selection mechanism to respond to changes in the evolving population without modifying the basic evolutionary framework of NSGA-II.

Experimental results on the DTLZ, WFG, and MaF test suites demonstrate that DES-NSGA-II achieves competitive IGD and $IGD^+$ performance across different problem structures and objective dimensions. The ablation results further show that the effects of adaptive selection-pressure regulation and hierarchical niching are strongly dependent on the problem structure and objective dimensionality. On DTLZ2, the advantage of the complete configuration becomes more evident as the number of objectives increases, whereas the contribution of the distributional-disturbance signal is relatively limited in some dimensions. On WFG4, the performance differences among configurations are less consistent, with simplified variants performing competitively on some instances but becoming substantially less effective at higher dimensions. On MaF3, the adaptive pressure regulation and hierarchical niching mechanisms have a more pronounced impact on high-dimensional and structurally complex instances, while simplified configurations can perform better in low-dimensional cases. These observations indicate that the proposed components do not provide uniform benefits across all optimization scenarios; rather, their effectiveness depends on the interaction between population characteristics, Pareto-front structure, and objective dimensionality.

Despite these results, several limitations remain. The current performance is still dependent on the characteristics of the optimization problem, and the regulation of $\beta_t$ relies on a heuristic formulation of the population-state indicators. Second, the current comparison does not include classical reference-point or reference-vector baselines such as NSGA-III or RVEA. Although the proposed mechanism targets the intensity of environmental selection rather than the reference frame itself, a

direct empirical comparison with these methods on high-dimensional regular fronts will be included in our future benchmark evaluations. Future work will also investigate more adaptive or parameter-free mechanisms for estimating selection pressure and explore alternative population-state descriptors to improve the generalization of dynamic environmental selection across different many-objective problems. In addition, the proposed environmental-selection strategy can be further evaluated on real-world many-objective optimization applications to examine its practical effectiveness and computational robustness.

## Author contributions

Renyun Liu: Conceptualization, Methodology, Writing–original draft, Supervision; Siyi Gong: Methodology, Software, Validation, Writing–review and editing; Du Cheng: Investigation, Visualization, Data curation; Rui Bao: Software, Formal analysis, Resources; Yifei Yao: Validation, Writing–review and editing, Funding acquisition. All authors have read and approved the final manuscript.

## Use of Generative-AI tools declaration

The authors declare that they have not used Artificial Intelligence (AI) tools in the creation of this article.

## Acknowledgments

This work was supported by the Jilin Scientific and Technological Development Program, China (Grant No. 20250201080GX).

## Conflict of interest

All authors declare no conflicts of interest in this paper.

## References

1. B. Li, J. Li, K. Tang, X. Yao, Many-objective evolutionary algorithms: A survey, *ACM Comput. Surv.*, **48** (2015), A10. https://doi.org/10.1145/2792984
2. K. Li, R. Wang, T. Zhang, H. Ishibuchi, Evolutionary many-objective optimization: A comparative study of the state-of-the-art, *IEEE Access*, **6** (2018), 26194–26214. https://doi.org/10.1109/ACCESS.2018.2832181
3. C. von Lücken, B. Barán, C. Brizuela, A survey on multi-objective evolutionary algorithms for many-objective problems, *Comput. Optim. Appl.*, **58** (2014), 707–756. https://doi.org/10.1007/s10589-014-9644-1
4. K. Deb, A. Pratap, S. Agarwal, T. Meyarivan, A fast and elitist multiobjective genetic algorithm: NSGA-II, *IEEE Trans. Evol. Comput.*, **6** (2002), 182–197. https://doi.org/10.1109/4235.996017

5. K. Deb, H. Jain, An evolutionary many-objective optimization algorithm using reference-point-based nondominated sorting approach, Part I: Solving problems with box constraints, *IEEE Trans. Evol. Comput.*, **18** (2014), 577–601. https://doi.org/10.1109/TEVC.2013.2281535
6. K. Deb, H. Jain, An evolutionary many-objective optimization algorithm using reference-point-based nondominated sorting approach, Part II: Handling constraints and extending to an adaptive approach, *IEEE Trans. Evol. Comput.*, **18** (2014), 602–622. https://doi.org/10.1109/TEVC.2013.2281534
7. R. Cheng, Y. Jin, M. Olhofer, B. Sendhoff, A reference vector guided evolutionary algorithm for many-objective optimization, *IEEE Trans. Evol. Comput.*, **20** (2016), 773–791. https://doi.org/10.1109/TEVC.2016.2519378
8. Q. Zhang, H. Li, MOEA/D: A multiobjective evolutionary algorithm based on decomposition, *IEEE Trans. Evol. Comput.*, **11** (2007), 712–731. https://doi.org/10.1109/TEVC.2007.892759
9. K. Li, K. Deb, Q. Zhang, S. Kwong, An evolutionary many-objective optimization algorithm based on dominance and decomposition, *IEEE Trans. Evol. Comput.*, **19** (2015), 694–716. https://doi.org/10.1109/TEVC.2014.2373386
10. H. Chen, Y. Tian, W. Pedrycz, G. Wu, R. Wang, L. Wang, Hyperplane assisted evolutionary algorithm for many-objective optimization problems, *IEEE Trans. Cybern.*, **50** (2020), 3367–3380. https://doi.org/10.1109/TCYB.2019.2899225
11. Y. Liu, H. Ishibuchi, N. Masuyama, Y. Nojima, Adapting reference vectors and scalarizing functions by growing neural gas to handle irregular Pareto fronts, *IEEE Trans. Evol. Comput.*, **24** (2020), 439–453. https://doi.org/10.1109/TEVC.2019.2926151
12. Q. Liu, Y. Jin, M. Heiderich, T. Rodemann, G. Yu, An adaptive reference vector-guided evolutionary algorithm using growing neural gas for many-objective optimization of irregular problems, *IEEE Trans. Cybern.*, **52** (2022), 2698–2711. https://doi.org/10.1109/TCYB.2020.3020630
13. Q. Liu, Y. Jin, M. Heiderich, T. Rodemann, Coordinated adaptation of reference vectors and scalarizing functions in evolutionary many-objective optimization, *IEEE Trans. Syst. Man Cybern.: Syst.*, **53** (2023), 763–775. https://doi.org/10.1109/TSMC.2022.3187370
14. Y. Hua, Q. Liu, K. Hao, Y. Jin, A survey of evolutionary algorithms for multi-objective optimization problems with irregular Pareto fronts, *IEEE/CAA J. Autom. Sinica*, **8** (2021), 303–318. https://doi.org/10.1109/JAS.2021.1003817
15. X. Wang, Z. Xie, X. Zhou, X. Gu, A two-stage adaptive reference direction guided evolutionary algorithm with modified dominance relation for many-objective optimization, *Swarm Evol. Comput.*, **78** (2023), 101272. https://doi.org/10.1016/j.swevo.2023.101272
16. Y. Xu, F. Li, H. Zhang, W. Li, An adaptive reference vector guided many-objective optimization algorithm based on the Pareto front density estimation, *Swarm Evol. Comput.*, **88** (2024), 101601. https://doi.org/10.1016/j.swevo.2024.101601
17. Y. Sun, B. Xue, M. Zhang, G. G. Yen, A new two-stage evolutionary algorithm for many-objective optimization, *IEEE Trans. Evol. Comput.*, **23** (2019), 748–761. https://doi.org/10.1109/TEVC.2018.2882166

18. W. Li, Q. Niliang, L. Wang, Q. Jiang, Two-stage many-objective evolutionary algorithm: enhanced dominance relations and control mechanisms for separated balance, *Complex Intell. Syst.*, **10** (2024), 6509–6543. https://doi.org/10.1007/s40747-024-01505-0
19. Z. Wei, H. Wang, S. Wang, Z. Zhang, Z. Cui, F. Wang, et al., Many-objective evolutionary algorithm based on parallel distance for handling irregular Pareto fronts, *Swarm Evol. Comput.*, **86** (2024), 101539. https://doi.org/10.1016/j.swevo.2024.101539
20. M. He, H. Zheng, H. Chen, Z. Wang, X. Liu, Y. Xia, et al., A clustering and vector angle-based adaptive evolutionary algorithm for multi-objective optimization with irregular Pareto fronts, *J. Supercomput.*, **81** (2025), 98. https://doi.org/10.1007/s11227-024-06496-w
21. M. He, X. Wang, H. Chen, X. Li, A knee point-driven many-objective evolutionary algorithm with adaptive switching mechanism, *J. Appl. Math.*, **2024** (2024), 4737604. https://doi.org/10.1155/2024/4737604
22. Z. Liu, F. Han, Q. Ling, H. Han, J. Jiang, Constraint-Pareto dominance and diversity enhancement strategy-based evolutionary algorithm for solving constrained multiobjective optimization problems, *IEEE Trans. Evol. Comput.*, **29** (2025), 2771–2784. https://doi.org/10.1109/TEVC.2024.3525153
23. Y. Tian, R. Cheng, X. Zhang, Y. Jin, PlatEMO: A MATLAB platform for evolutionary multi-objective optimization, *IEEE Comput. Intell. Mag.*, **12** (2017), 73–87. https://doi.org/10.1109/MCI.2017.2742868
24. L. R. C. de Farias, A. F. R. Araújo, IM-MOEA/D: An inverse modeling multi-objective evolutionary algorithm based on decomposition, In: *2021 IEEE International Conference on Systems, Man, and Cybernetics (SMC)*, (2021), 462–467. https://doi.org/10.1109/SMC52423.2021.9658650
25. C. He, R. Cheng, L. Li, K. C. Tan, Y. Jin, Large-scale multiobjective optimization via reformulated decision variable analysis, *IEEE Trans. Evol. Comput.*, **28** (2024), 47–61. https://doi.org/10.1109/TEVC.2022.3213006
26. Y. Hua, Q. Liu, K. Hao, Adaptive normal vector guided evolutionary multi- and many-objective optimization, *Complex Intell. Syst.*, **10** (2024), 3709–3726. https://doi.org/10.1007/s40747-024-01353-y
27. X. Yang, J. Zou, S. Yang, J. Zheng, Y. Liu, A fuzzy decision variables framework for large-scale multiobjective optimization, *IEEE Trans. Evol. Comput.*, **27** (2023), 445–459. https://doi.org/10.1109/TEVC.2021.3118593
28. Z. Liu, F. Han, Q. Ling, H. Han, J. Jiang, A many-objective optimization evolutionary algorithm based on hyper-dominance degree, *Swarm Evol. Comput.*, **83** (2023), 101411. https://doi.org/10.1016/j.swevo.2023.101411
29. Y. Tian, L. Si, X. Zhang, K. C. Tan, Y. Jin, Local model based Pareto front estimation for multi-objective optimization, *IEEE Trans. Syst., Man, Cybern.: Syst.*, **53** (2023), 623–634. https://doi.org/10.1109/TSMC.2022.3186546
30. C. He, R. Cheng, D. Yazdani, Adaptive offspring generation for evolutionary large-scale multiobjective optimization, *IEEE Trans. Syst., Man, Cybern.: Syst.*, **52** (2022), 786–798. https://doi.org/10.1109/TSMC.2020.3003926

31. L. Pan, W. Xu, L. Li, C. He, R. Cheng, Adaptive simulated binary crossover for rotated multi-objective optimization, *Swarm Evol. Comput.*, **60** (2021), 100759. https://doi.org/10.1016/j.swevo.2020.100759

32. K. Deb, R. B. Agrawal, Simulated binary crossover for continuous search space, *Complex Syst.*, **9** (1995), 115–148.

33. K. Deb, M. Goyal, A combined genetic adaptive search (GeneAS) for engineering design, *Comput. Sci. Inform.*, **26** (1996), 30–45.

34. E. Zitzler, L. Thiele, M. Laumanns, C. M. Fonseca, V. Grunert da Fonseca, Performance assessment of multiobjective optimizers: An analysis and review, *IEEE Trans. Evol. Comput.*, **7** (2003), 117–132. https://doi.org/10.1109/TEVC.2003.810758

35. H. Ishibuchi, H. Masuda, Y. Tanigaki, Y. Nojima, Modified distance calculation in generational distance and inverted generational distance, In: *Evolutionary Multi-Criterion Optimization (EMO 2015, LNCS 9018)*, (2015), 110–125. https://doi.org/10.1007/978-3-319-15892-1_8

36. J. Demšar, Statistical comparisons of classifiers over multiple data sets, *J. Mach. Learn. Res.*, **7** (2006), 1–30.

37. L. L. Peng, T. Li, G. F. Fan, X. Y. Yang, W. C. Hong, Short-term electric load forecasting by cross-feature analysis and multimodal selection, *Comput. Model. Eng. Sci.*, **149** (2026), 1–10. https://doi.org/10.32604/cmes.2026.087031

38. L. L. Peng, X. Y. Yang, X. X. Hua, G. F. Fan, Y. J. Wang, A. J. Umbarkar, et al., Short-term electric load forecasting based on deep learning and multi-modal fusion, *Electr. Power Syst. Res.*, **254** (2026), 112593. https://doi.org/10.1016/j.epsr.2025.112593




AIMS Press

© 2026 the Author(s), licensee AIMS Press. This is an open access article distributed under the terms of the Creative Commons Attribution License (https://creativecommons.org/licenses/by/4.0)